Complex-amplitude metasurfaces for holography and fiber optics implemented via direct laser writing

Nanolight 2022, Benasque, March 11 2022

Stefan A Maier

Chair in Hybrid Nanosystems, Nanoinstitut München, LMU München

Lee Lucas Chair in Experimental Physics, Imperial College London

Stefan.Maier@physik.uni-muenchen.de

www.hybridplasmonics.org

Meta-optics: Metasurfaces and metafibers

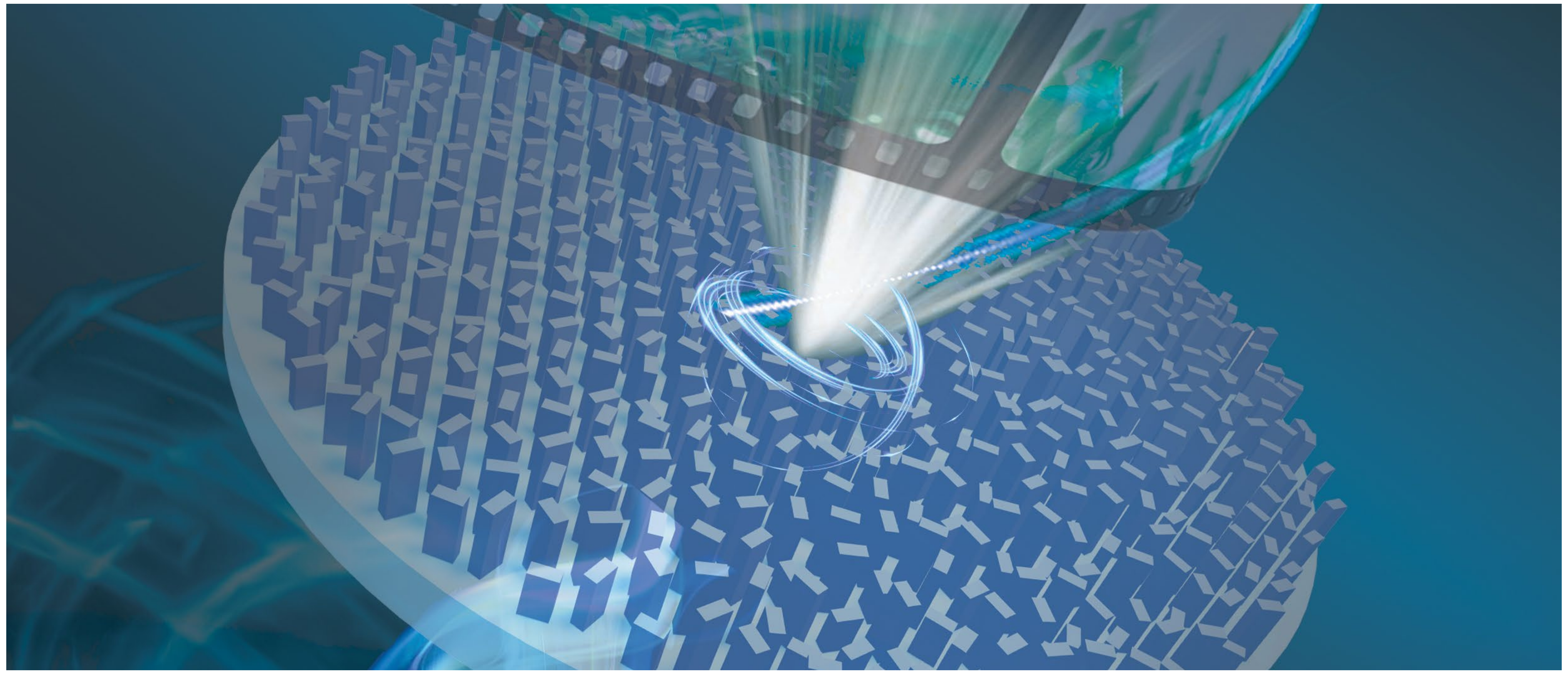

Holography

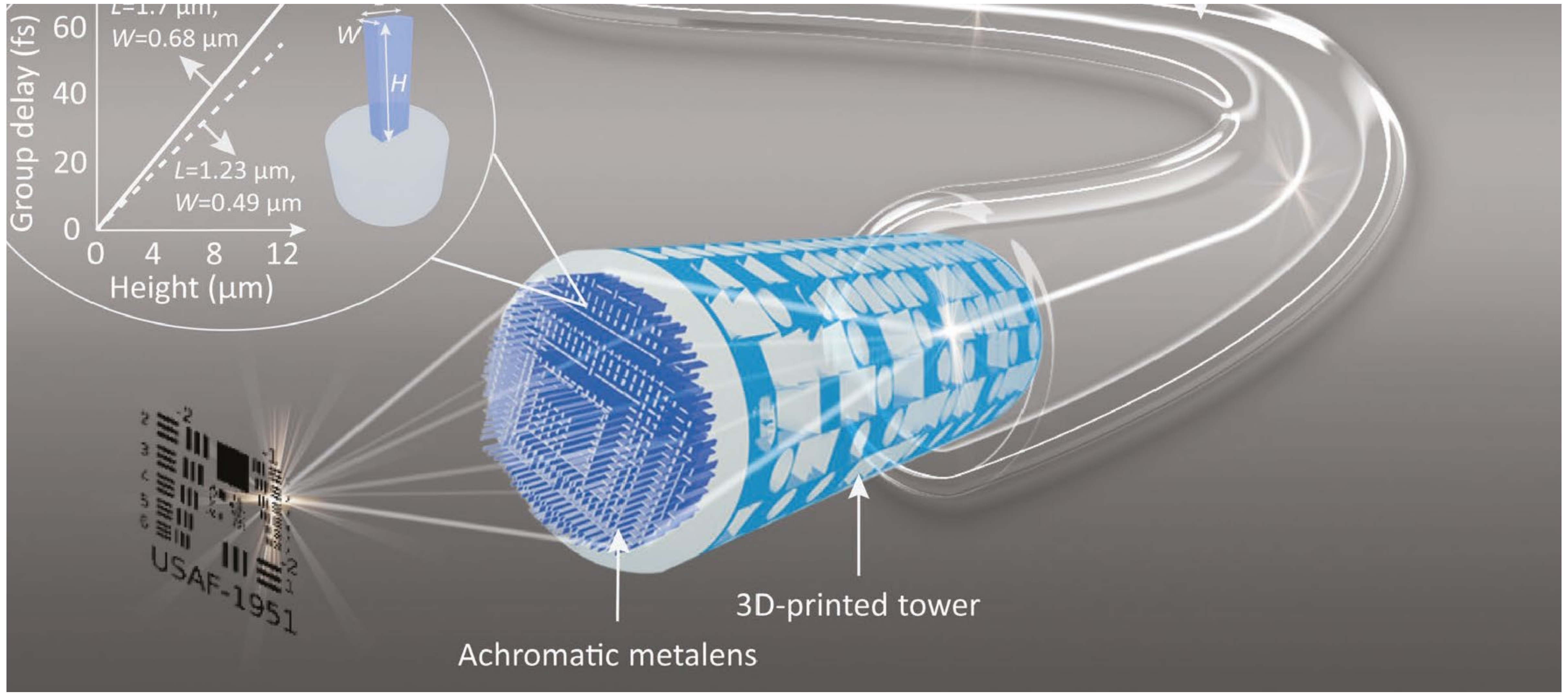

Telecommunications and fiber optics

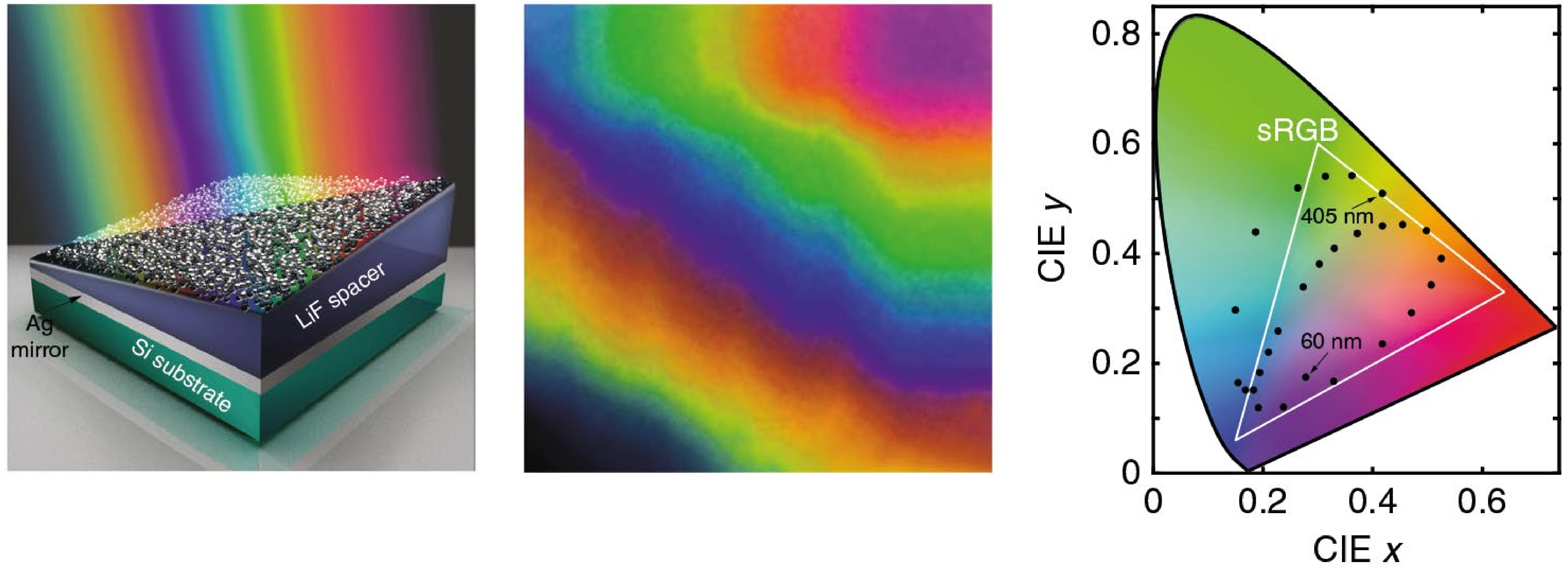

Light harvesting with disordered systems

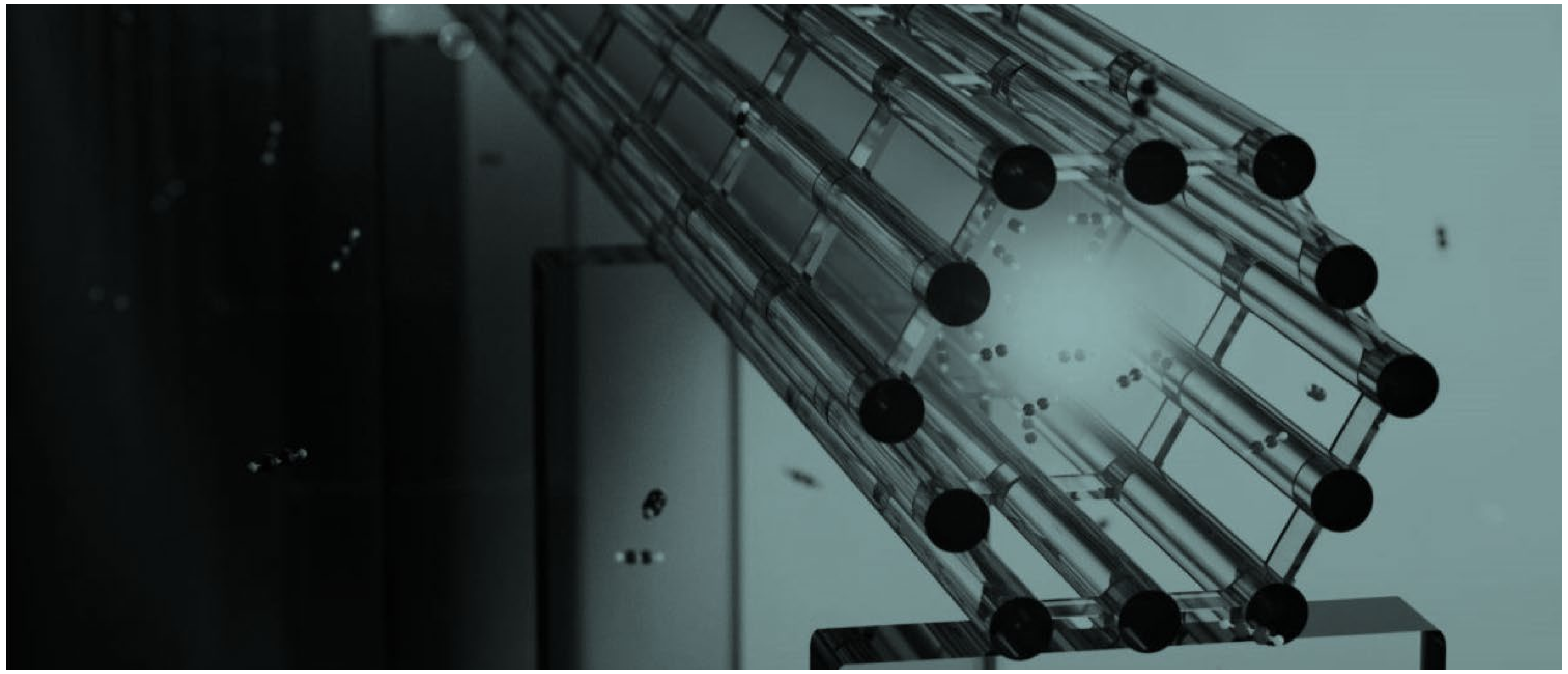

Light cages for sensing and spectroscopy

Outline

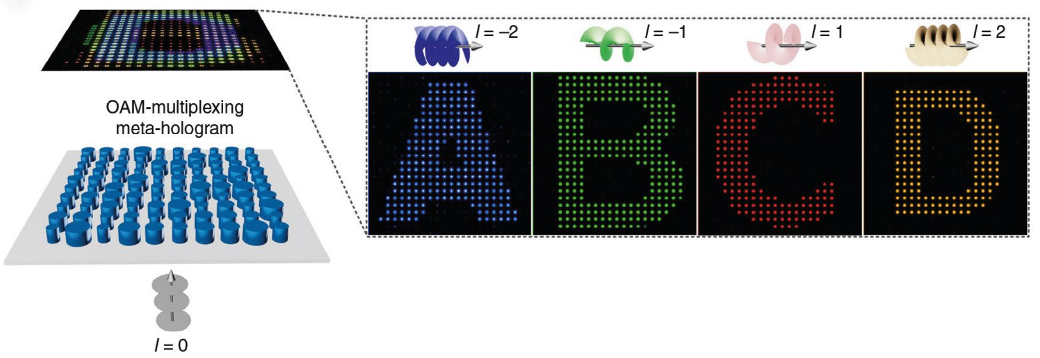

Metasurface holography

Nature Nanotechnology **15**, 948 (2020)
Nature Communications **10**, 2986 (2019)

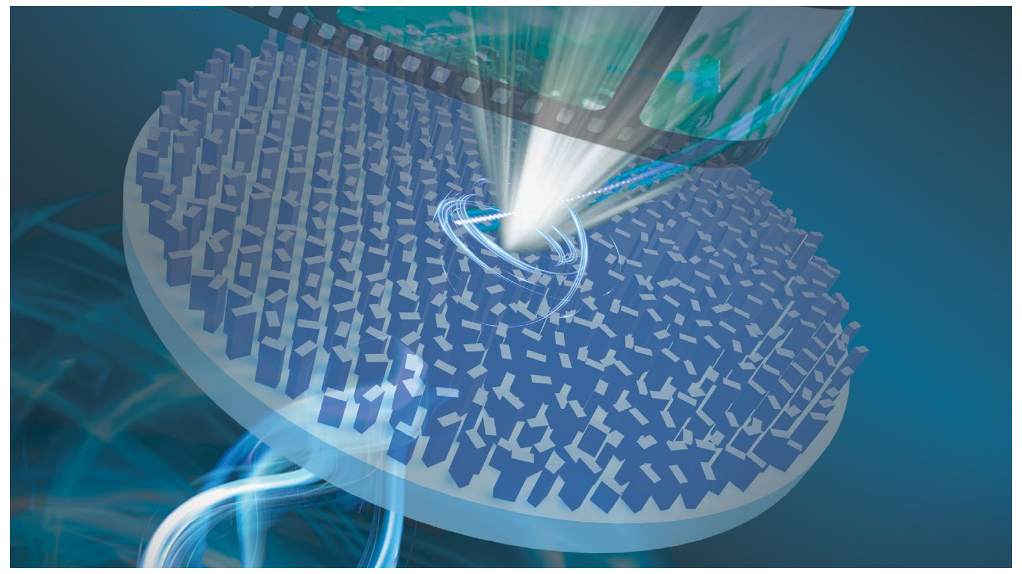

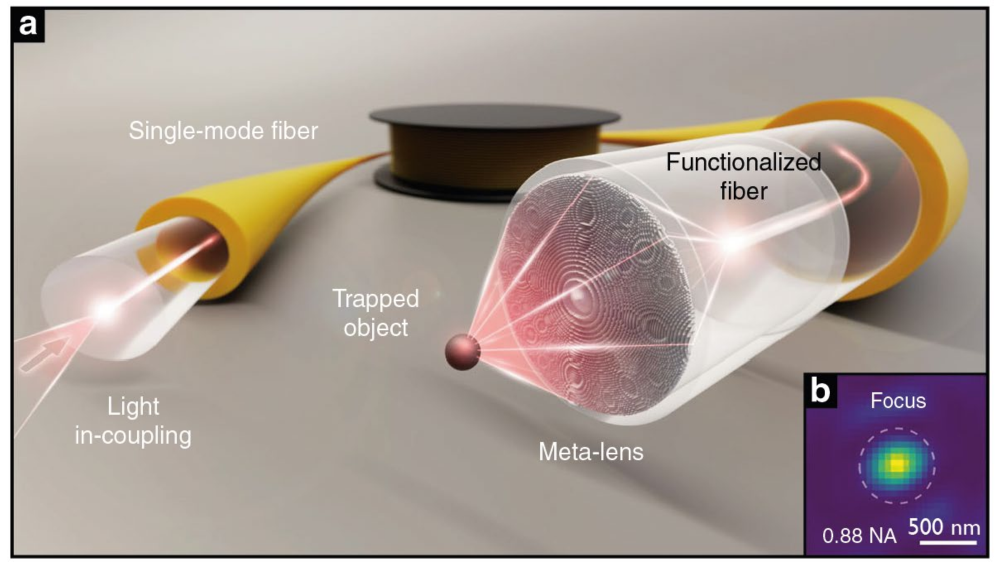

Meta-optics for optical fibre applications

*arxiv.org/abs/***2201.07158**
Light: Science & Applications **10:57** (2021)

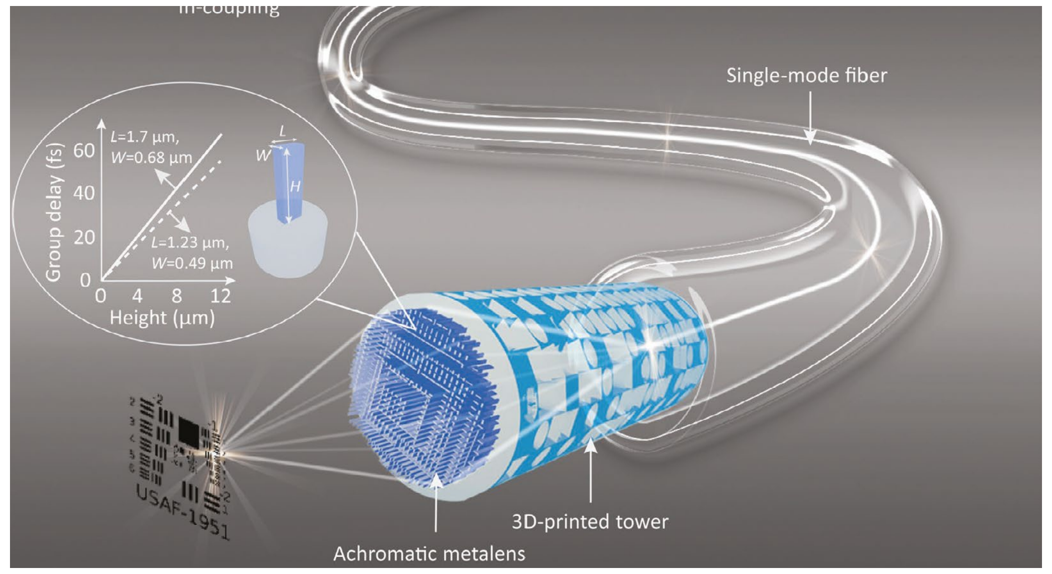

Outline

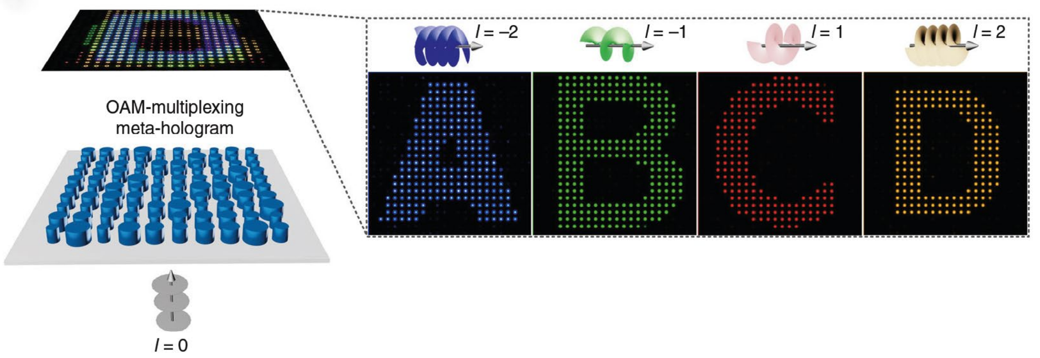

Metasurface holography

Nature Nanotechnology **15**, 948 (2020)
Nature Communications **10**, 2986 (2019)

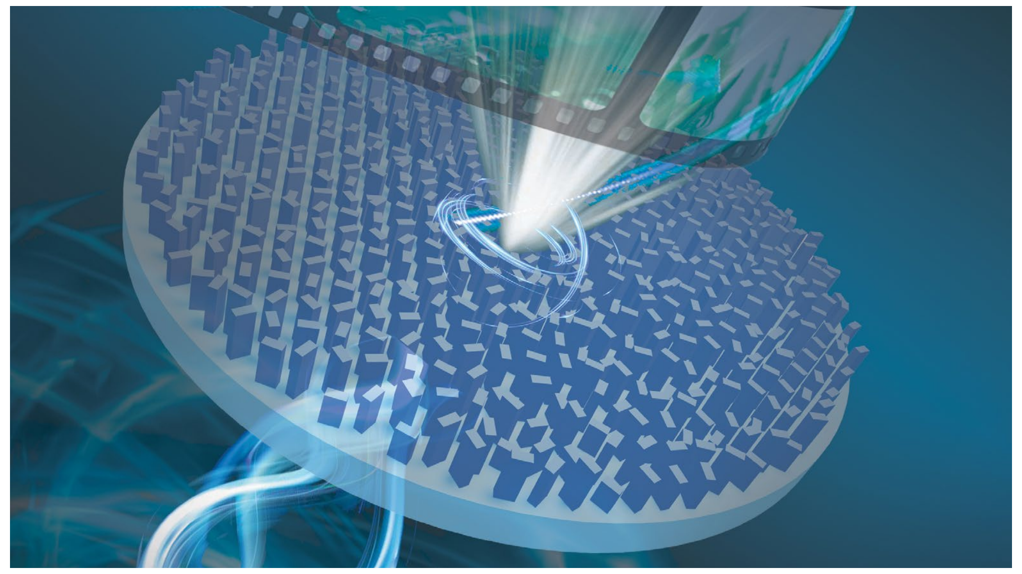

Meta-optics for optical fibre applications

*arxiv.org/abs/*2201.07158
Light: Science & Applications **10**:57 (2021)

Wavefront manipulation via metasurfaces

Light Propagation with Phase Discontinuities: Generalized Laws of Reflection and Refraction

Nanfang Yu,[1] Patrice Genevet,[1,2] Mikhail A. Kats,[1] Francesco Aieta,[1,3] Jean-Philippe Tetienne,[1,4] Federico Capasso,[1*] Zeno Gaburro[1,5*]

Conventional optical components rely on gradual phase shifts accumulated during light propagation to shape light beams. New degrees of freedom are attained by introducing abrupt phase changes over the scale of the wavelength. A two-dimensional array of optical resonators with spatially varying phase response and subwavelength separation can imprint such phase discontinuities on propagating light as it traverses the interface between two media. Anomalous reflection and refraction phenomena are observed in this regime in optically thin arrays of metallic antennas on silicon with a linear phase variation along the interface, which are in excellent agreement with generalized laws derived from Fermat's principle. Phase discontinuities provide great flexibility in the design of light beams, as illustrated by the generation of optical vortices through use of planar designer metallic interfaces.

The shaping of the wavefront of light with optical components such as lenses and prisms, as well as diffractive elements such as gratings and holograms, relies on gradual phase changes accumulated along the optical path. This approach is generalized in transformation optics (*1*, *2*), which uses metamaterials to bend light in unusual ways, achieving such phenomena as negative refraction, subwavelength-focusing, and cloaking (*3*, *4*) and even to explore unusual geometries of space-time in the early universe (*5*). A new degree of freedom of controlling wavefronts can be attained by introducing abrupt phase shifts over the scale of the wavelength along the optical path, with the propagation of light governed by Fermat's principle. The latter states that the trajectory taken between two points A and B by a ray of light is that of the least optical path, $\int_A^B n(\vec{r})dr$, where $n(\vec{r})$ is the local index of refraction, and readily gives the laws of reflection and refraction between two media. In its most general form, Fermat's principle can be stated as the principle of stationary phase (*6*–*8*); that is, the derivative of the phase $\int_A^B d\varphi(\vec{r})$ accumulated along the actual light path will be zero with respect to infinitesimal variations of the path. We show that an abrupt phase shift $\Phi(\vec{r}_s)$ over the scale of the wavelength can be introduced in the optical path by suitably engineering the interface between two media; $\Phi(\vec{r}_s)$ depends on the coordinate $\vec{r}_s$ along the interface. Then, the total phase shift $\Phi(\vec{r}_s) + \int_A^B \vec{k} \cdot d\vec{r}$ will be stationary for the actual path that light takes; $\vec{k}$ is the wave vector of the propagating light. This provides a generalization of the laws of reflection and refraction, which is applicable to a wide range of subwavelength structured interfaces between two media throughout the optical spectrum.

Generalized laws of reflection and refraction. The introduction of an abrupt phase shift, denoted as phase discontinuity, at the interface between two media allows us to revisit the laws of reflection and refraction by applying Fermat's principle. Consider an incident plane wave at an angle θ_i. Assuming that the two paths are infinitesimally close to the actual light path (Fig. 1), then the phase difference between them is zero

$$[k_o n_i \sin(\theta_i)dx + (\Phi + d\Phi)] - [k_o n_t \sin(\theta_t)dx + \Phi] = 0 \quad (1)$$

where θ_t is the angle of refraction; Φ and $\Phi+d\Phi$ are, respectively, the phase discontinuities at the locations where the two paths cross the interface; dx is the distance between the crossing points; n_i and n_t are the refractive indices of the two media; and $k_o = 2\pi/\lambda_o$, where λ_o is the vacuum wavelength. If the phase gradient along the interface is designed to be constant, the previous equation leads to the generalized Snell's law of refraction

$$\sin(\theta_t)n_t - \sin(\theta_i)n_i = \frac{\lambda_o}{2\pi}\frac{d\Phi}{dx} \quad (2)$$

Equation 2 implies that the refracted beam can have an arbitrary direction, provided that a suitable constant gradient of phase discontinuity along the interface ($d\Phi/dx$) is introduced. Because of the nonzero phase gradient in this modified Snell's law, the two angles of incidence $\pm\theta_i$ lead to different values for the angle of refraction. As a consequence, there are two possible critical angles for total internal reflection, provided that $n_t < n_i$:

$$\theta_c = \arcsin\left(\pm\frac{n_t}{n_i} - \frac{\lambda_o}{2\pi n_i}\frac{d\Phi}{dx}\right) \quad (3)$$

Similarly, for reflection we have

$$\sin(\theta_r) - \sin(\theta_i) = \frac{\lambda_o}{2\pi n_i}\frac{d\Phi}{dx} \quad (4)$$

where θ_r is the angle of reflection. There is a nonlinear relation between θ_r and θ_i, which is markedly different from conventional specular reflection. Equation 4 predicts that there is always a critical angle of incidence

$$\theta_c' = \arcsin\left(1 - \frac{\lambda_o}{2\pi n_i}\left|\frac{d\Phi}{dx}\right|\right) \quad (5)$$

above which the reflected beam becomes evanescent.

In the above derivation, we have assumed that Φ is a continuous function of the position along the interface; thus, all the incident energy is transferred into the anomalous reflection and refraction. However, because experimentally we use an array of optically thin resonators with subwavelength separation to achieve the phase change along the interface, this discreteness implies that there are also regularly reflected and refracted beams, which follow conventional laws of reflection and refraction ($d\Phi/dx = 0$ in Eqs. 2 and 4). The separation between the resonators controls the amount of energy in the anomalously reflected and refracted beams. We have also assumed that the amplitudes of the scattered radiation by each resonator are identical, so that the reflected and refracted beams are plane waves. In the next section, we will show with simulations—which represent numerical solutions of Maxwell's

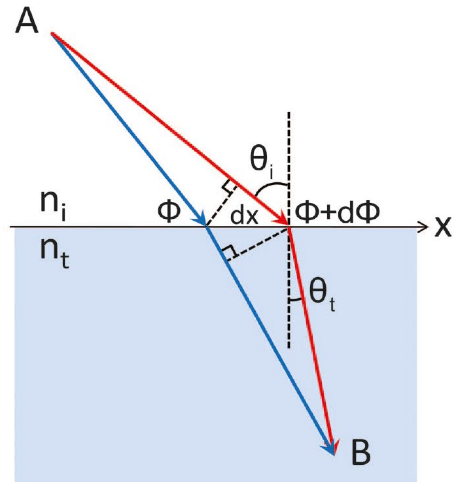

Fig. 1. Schematics used to derive the generalized Snell's law of refraction. The interface between the two media is artificially structured in order to introduce an abrupt phase shift in the light path, which is a function of the position along the interface. Φ and $\Phi + d\Phi$ are the phase shifts where the two paths (blue and red) cross the boundary.

[1]School of Engineering and Applied Sciences, Harvard University, Cambridge, MA 02138, USA. [2]Institute for Quantum Studies and Department of Physics, Texas A&M University, College Station, TX 77843, USA. [3]Dipartimento di Fisica e Ingegneria dei Materiali e del Territorio, Università Politecnica delle Marche, via Brecce Bianche, 60131 Ancona, Italy. [4]Laboratoire de Photonique Quantique et Moléculaire, Ecole Normale Supérieure de Cachan and CNRS, 94235 Cachan, France. [5]Dipartimento di Fisica, Università degli Studi di Trento, via Sommarive 14, 38100 Trento, Italy.

*To whom correspondence should be addressed. E-mail: capasso@seas.harvard.edu (F.C.); gaburro@seas.harvard.edu (Z.G.)

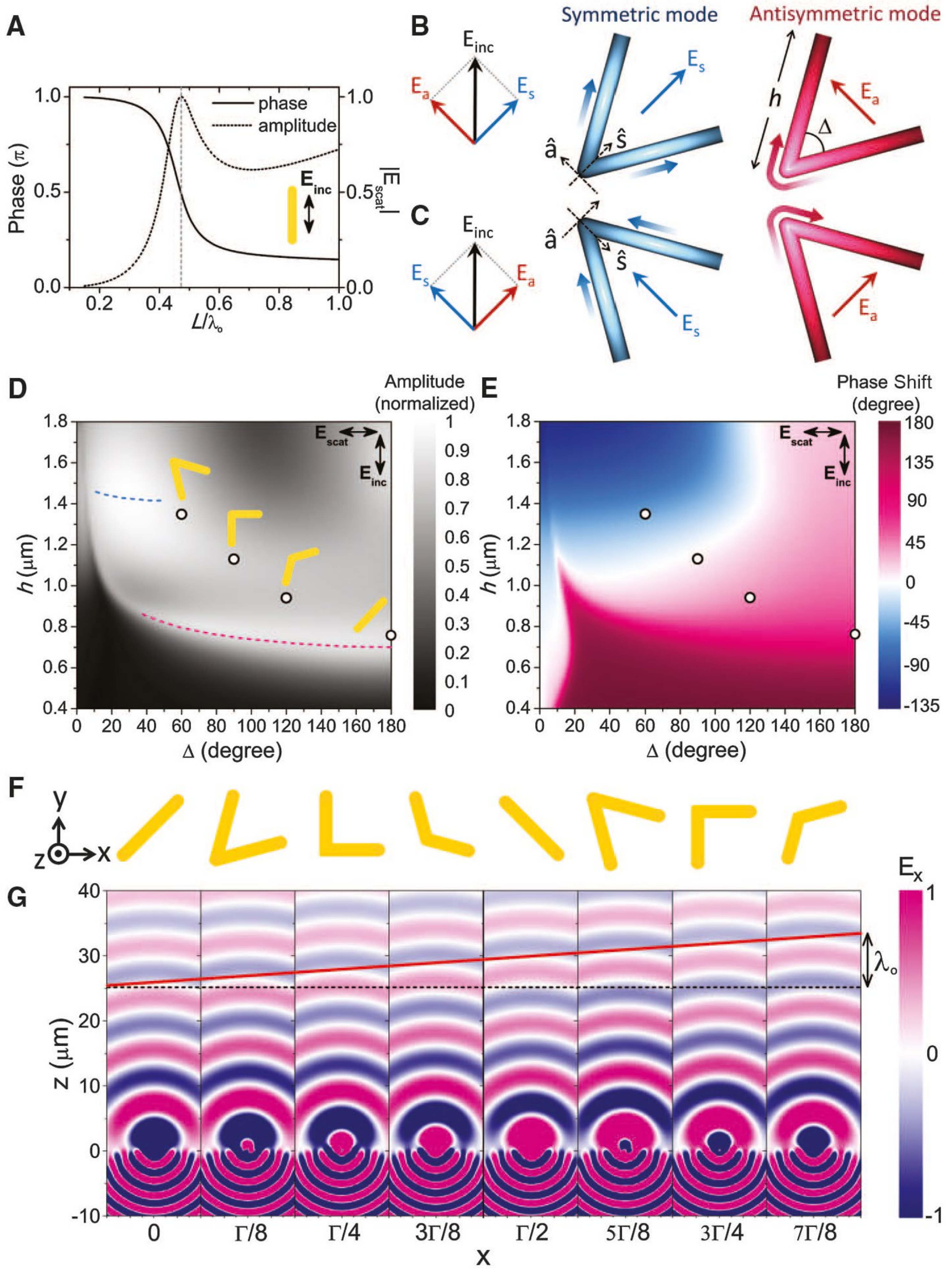

Steering light via sub-wavelength control over amplitude and phase manipulation

Beginnings of metasurface holography

Montelongo et al, Nano Letters **14**, 294 (2014)

Huang et al, Nature Communications **4**, 2808 (2013)

see e.g. review by Huang, Zhang and Zentgraf, *Nanophotonics* **7**, 1169 (2018)

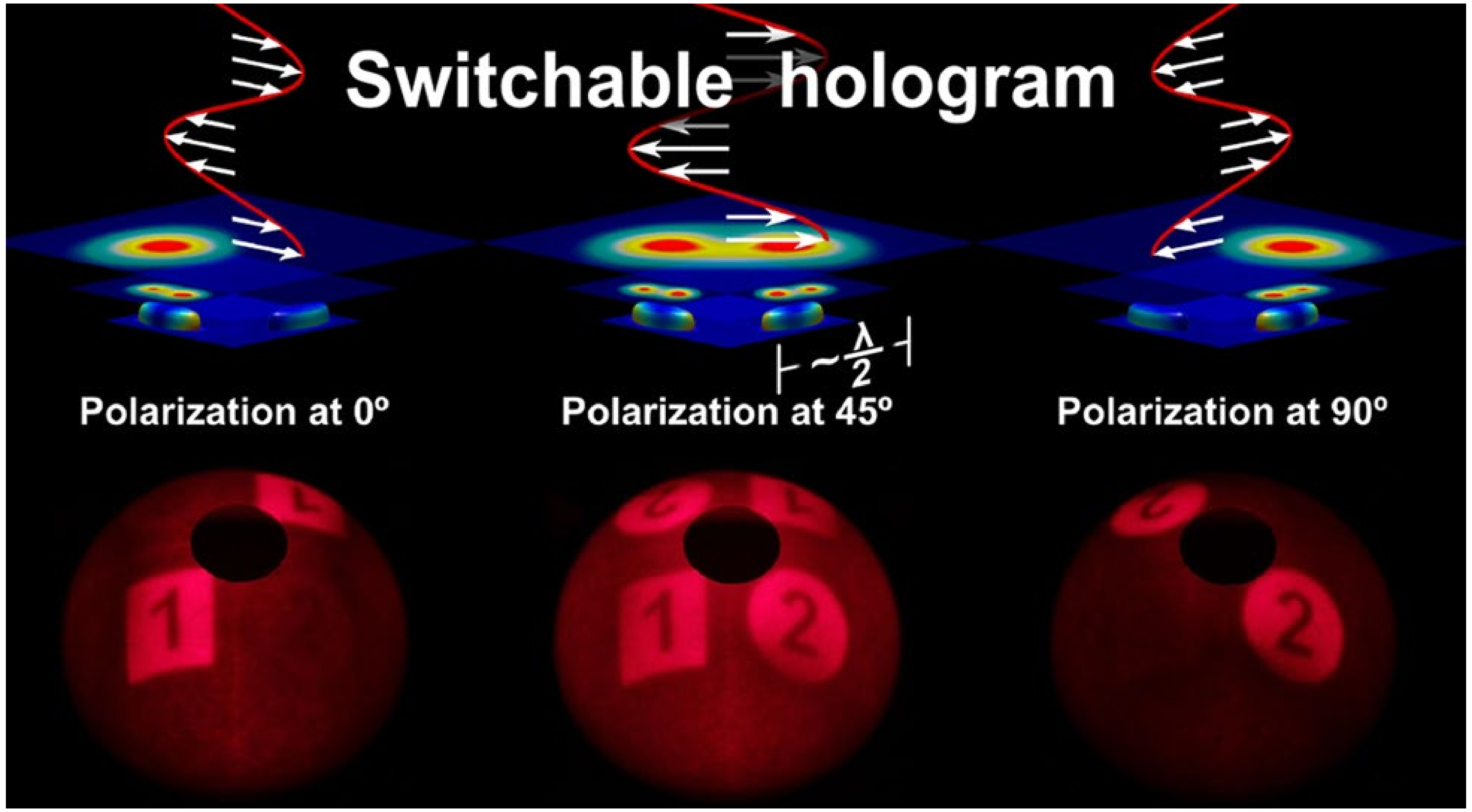

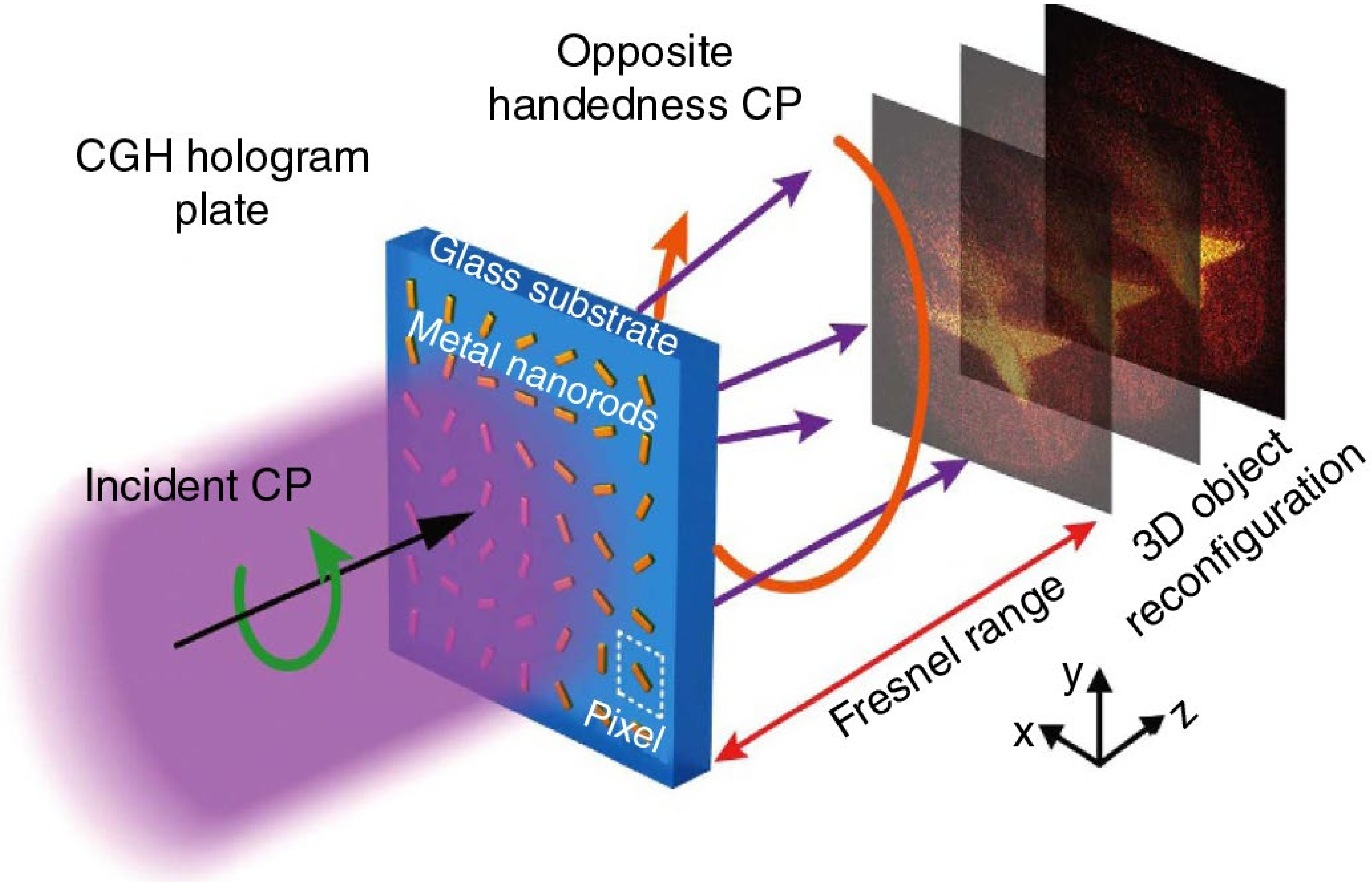

- digitization of holographic diffraction patterns via sub-wavelength nanoantennas enables reconstruction of high-resolution images with wide field of view
- superposition of independent transverse polarizations in a sub-wavelength distance with minimal cross talk
  ⇒ **result of highly anisotropic scattering response of nanoantenna**

- metasurfaces enable abrupt (dispersionless) interfacial phase changes and hence control over the local wave front on sub-wavelength scales
  ⇒ **encoding of phase information into surface structures acting as point sources in the context of computer-generated holography**
- uniform scattering amplitudes enable very simple generation of phase-only polarization-based metasurface holograms of diffuse-reflecting surfaces

Increasing information capacity via multiplexing

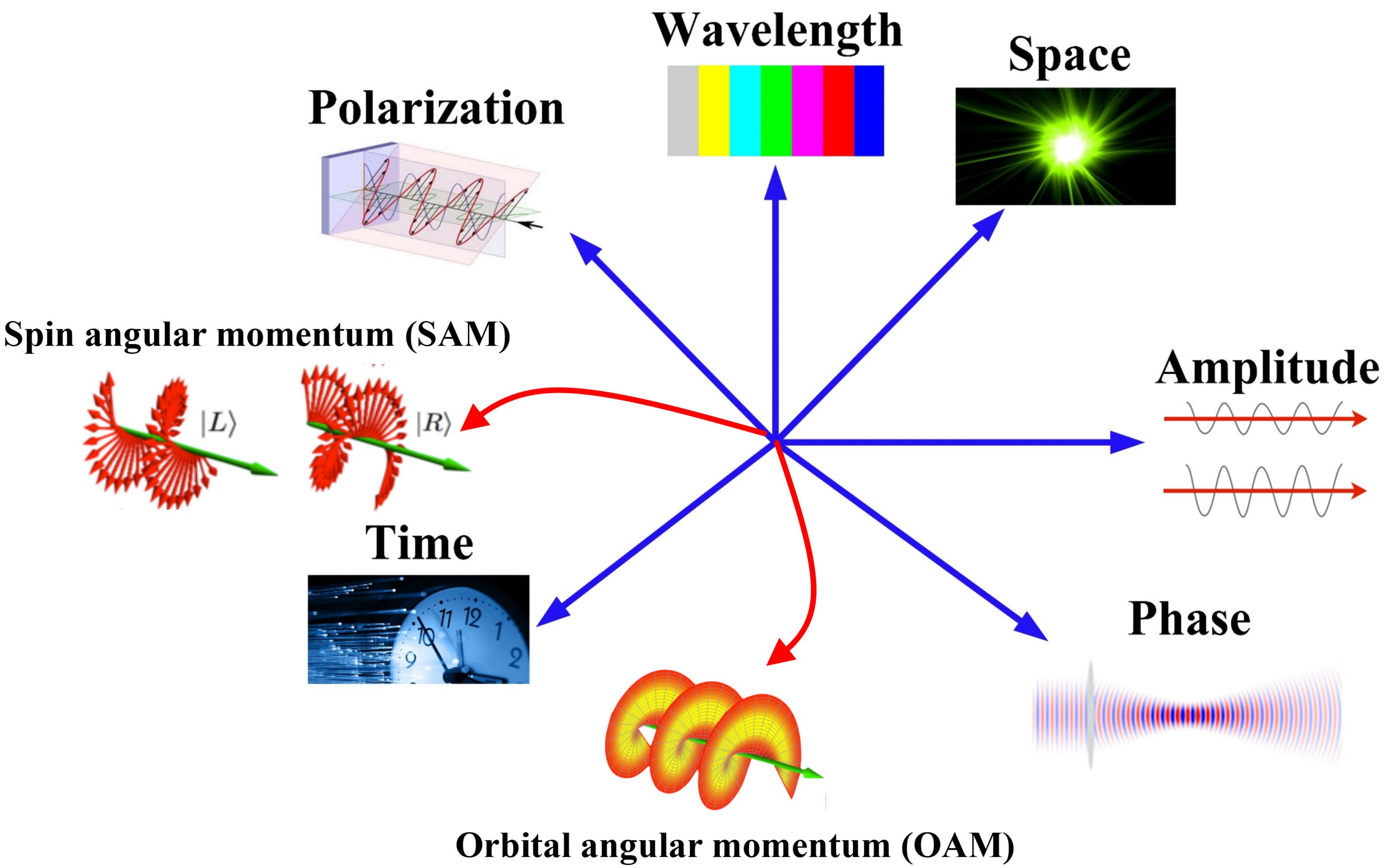

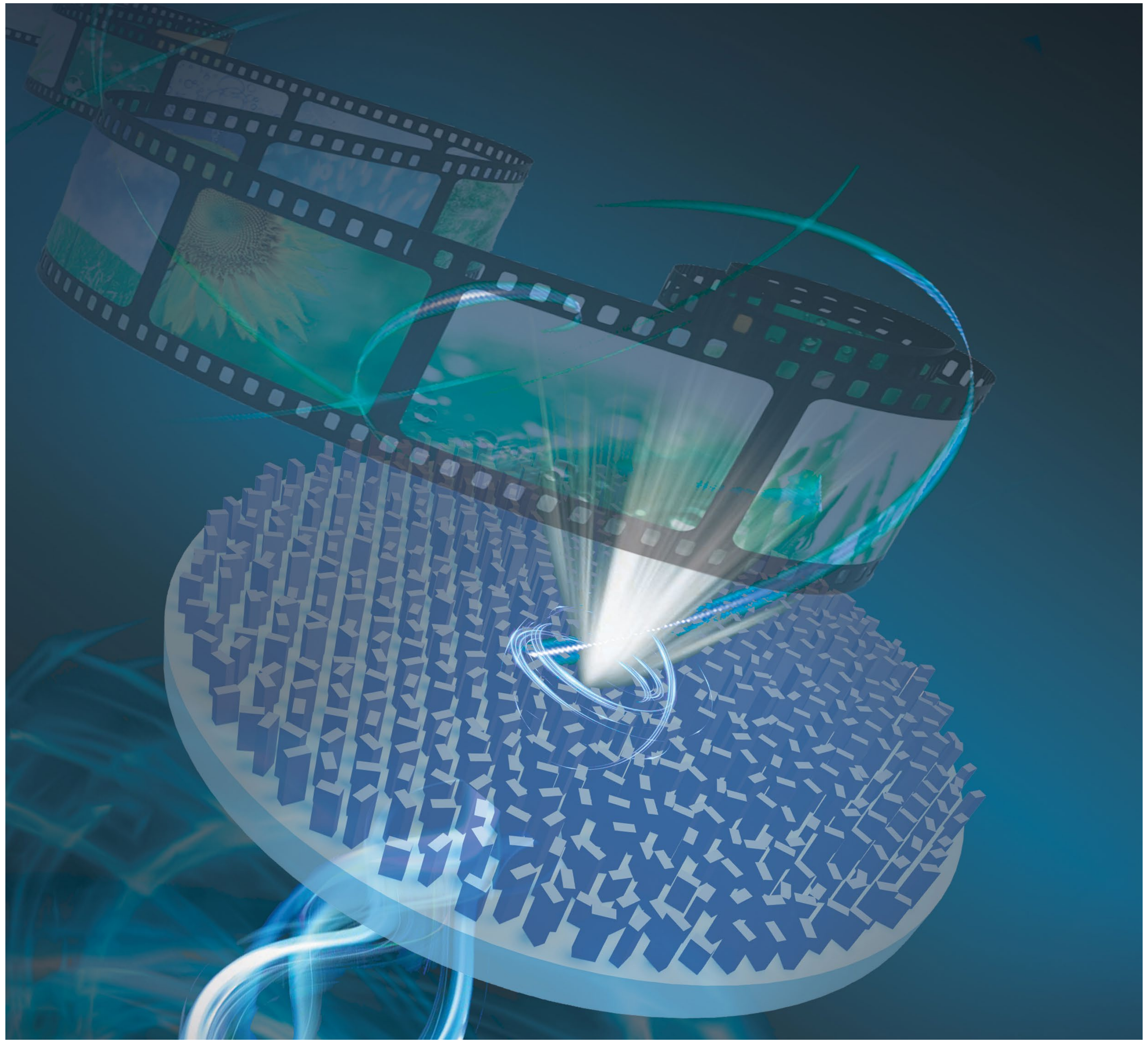

We focus on enhancing information-storage capabilities via the **orbital angular momentum** degree of freedom

Optical vortices and metasurfaces

Chinese Optics 14, 792 (2021)

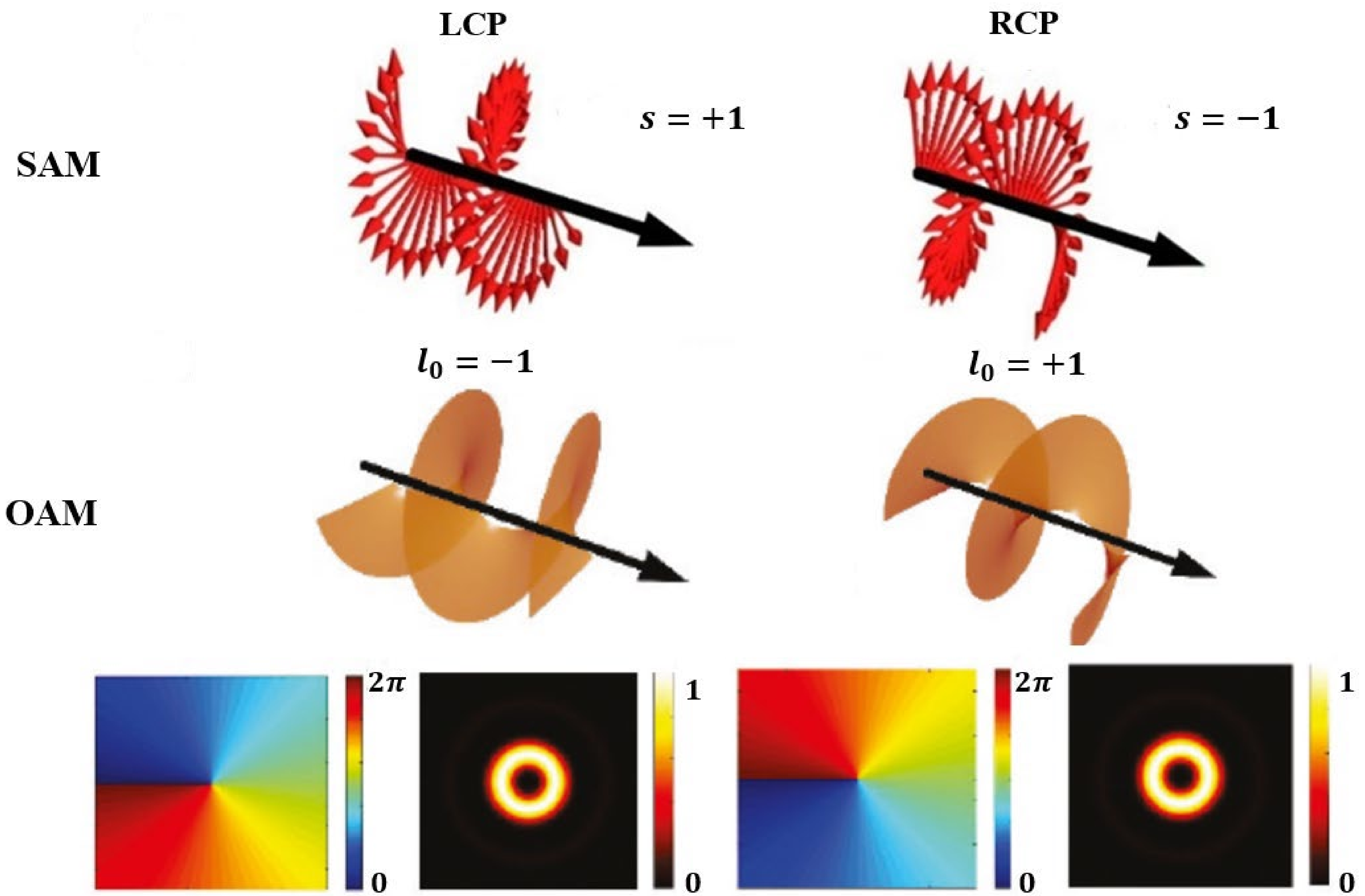

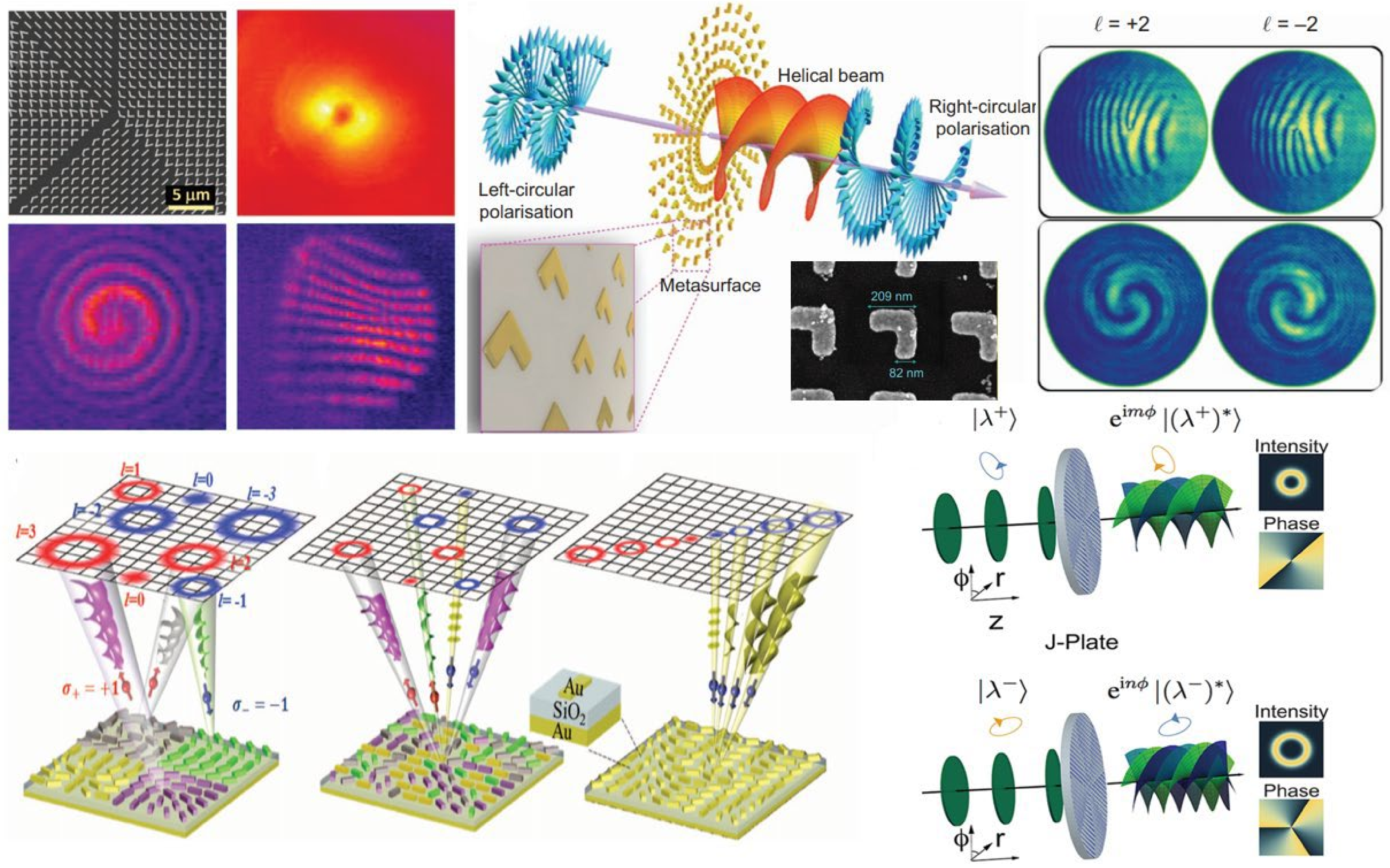

Preserving orbital angular momentum

Nature Communications **10**, 2986 (2019)

Conventional OAM non-preservative holography

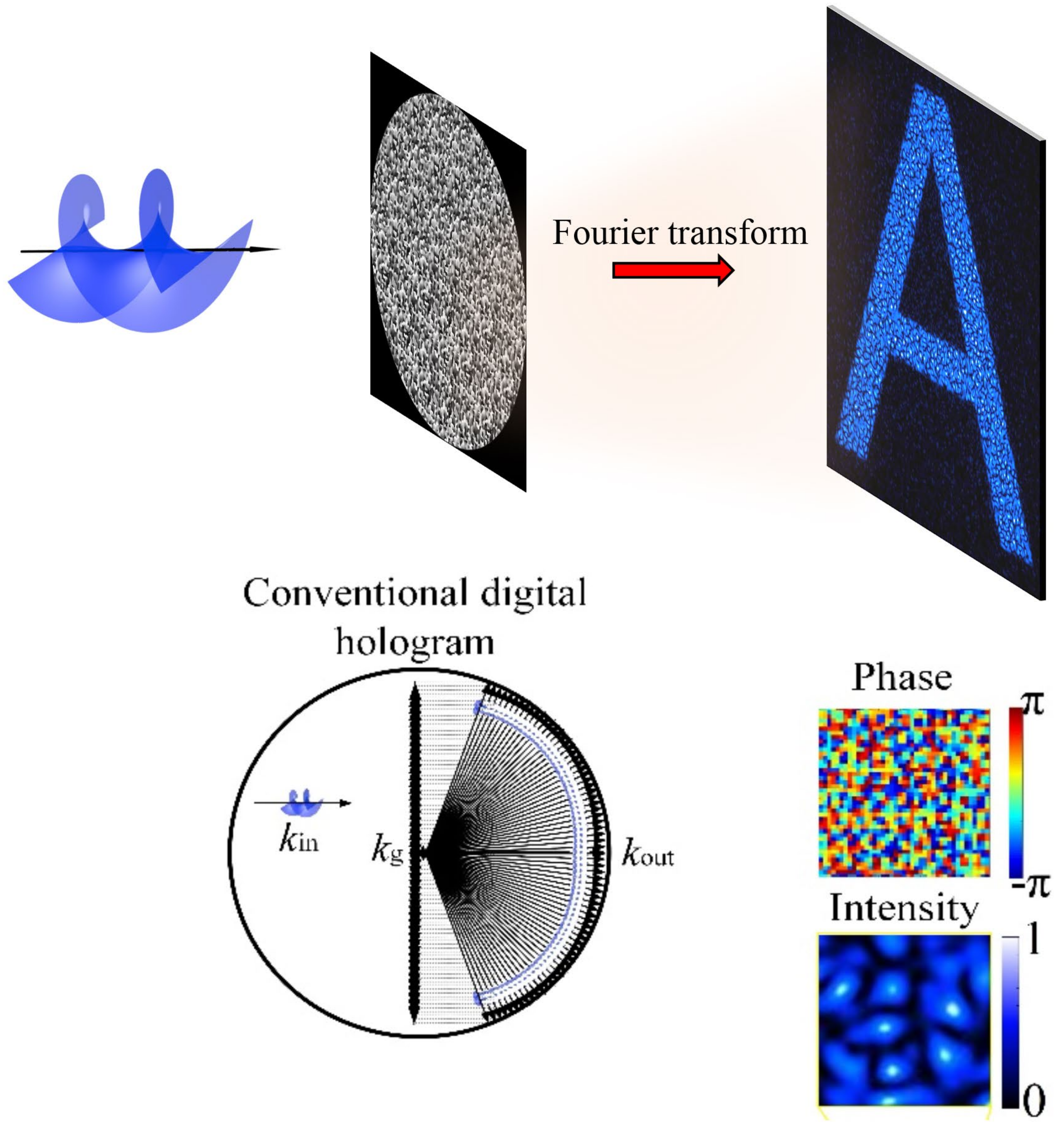

OAM-preserving holography

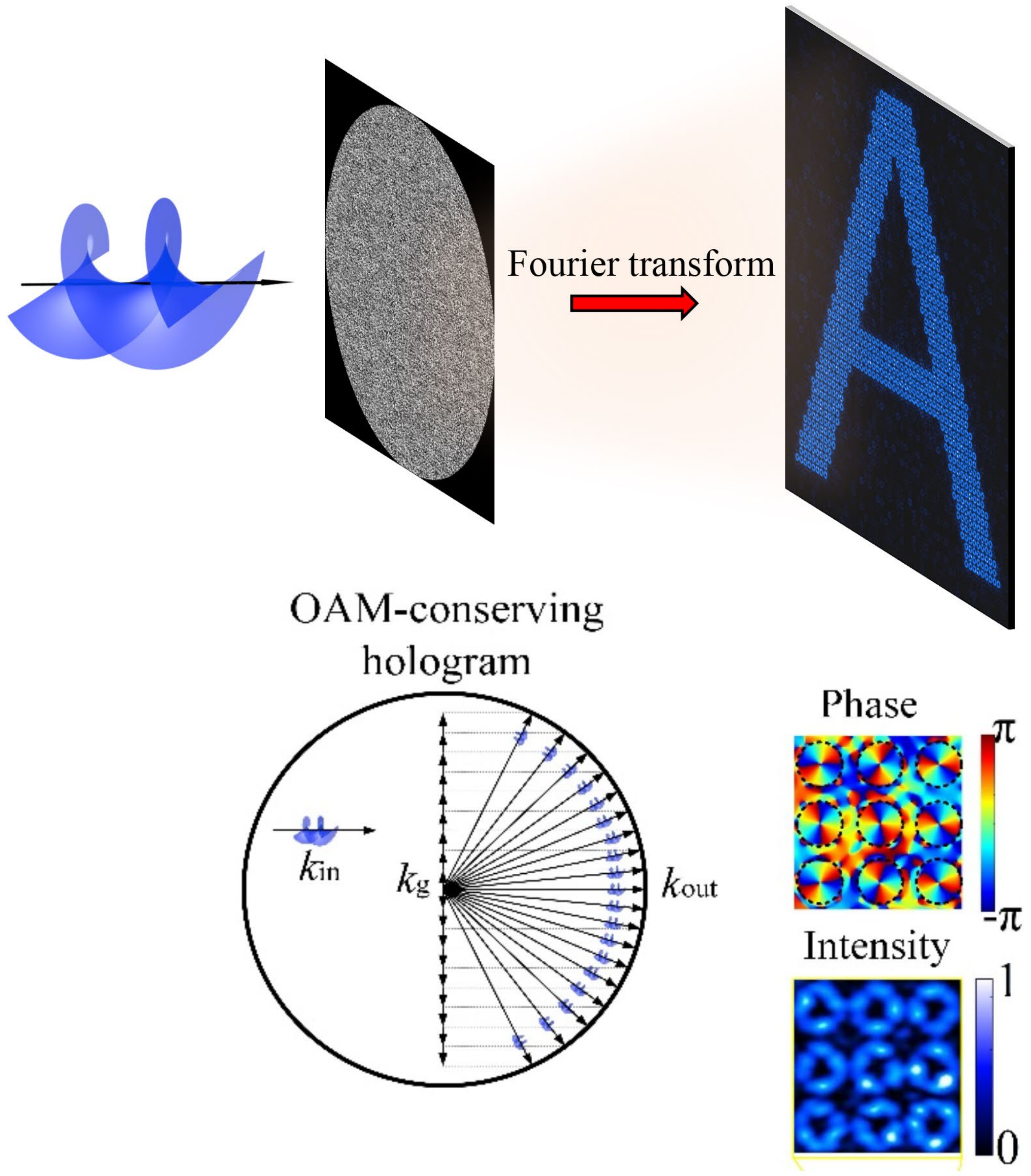

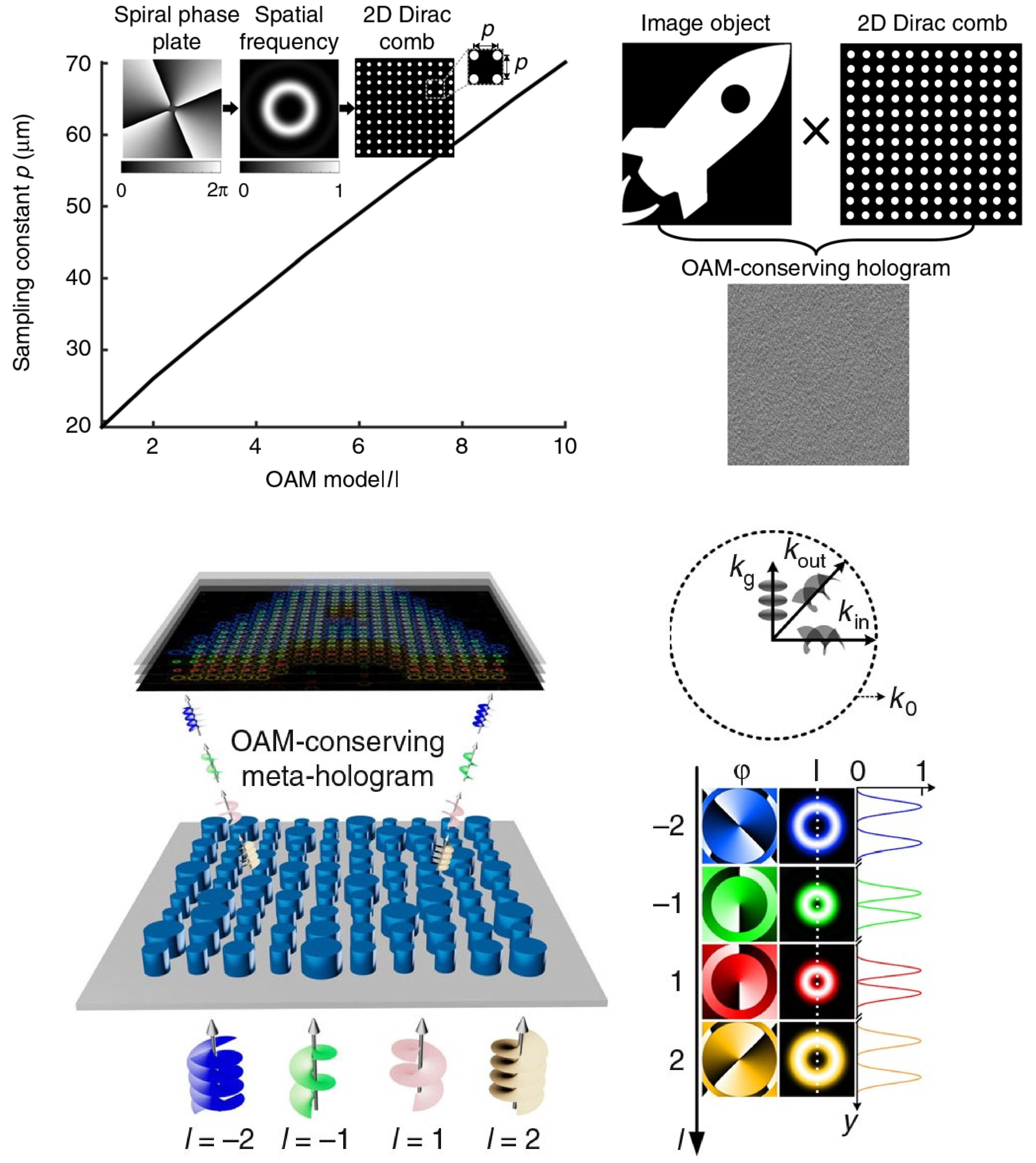

Change from quasi-continuous to topological-charge-dependent sampling period enables OAM-pixelated holographic images

Selecting for a specific orbital angular momentum

Nature Communications **10**, 2986 (2019)

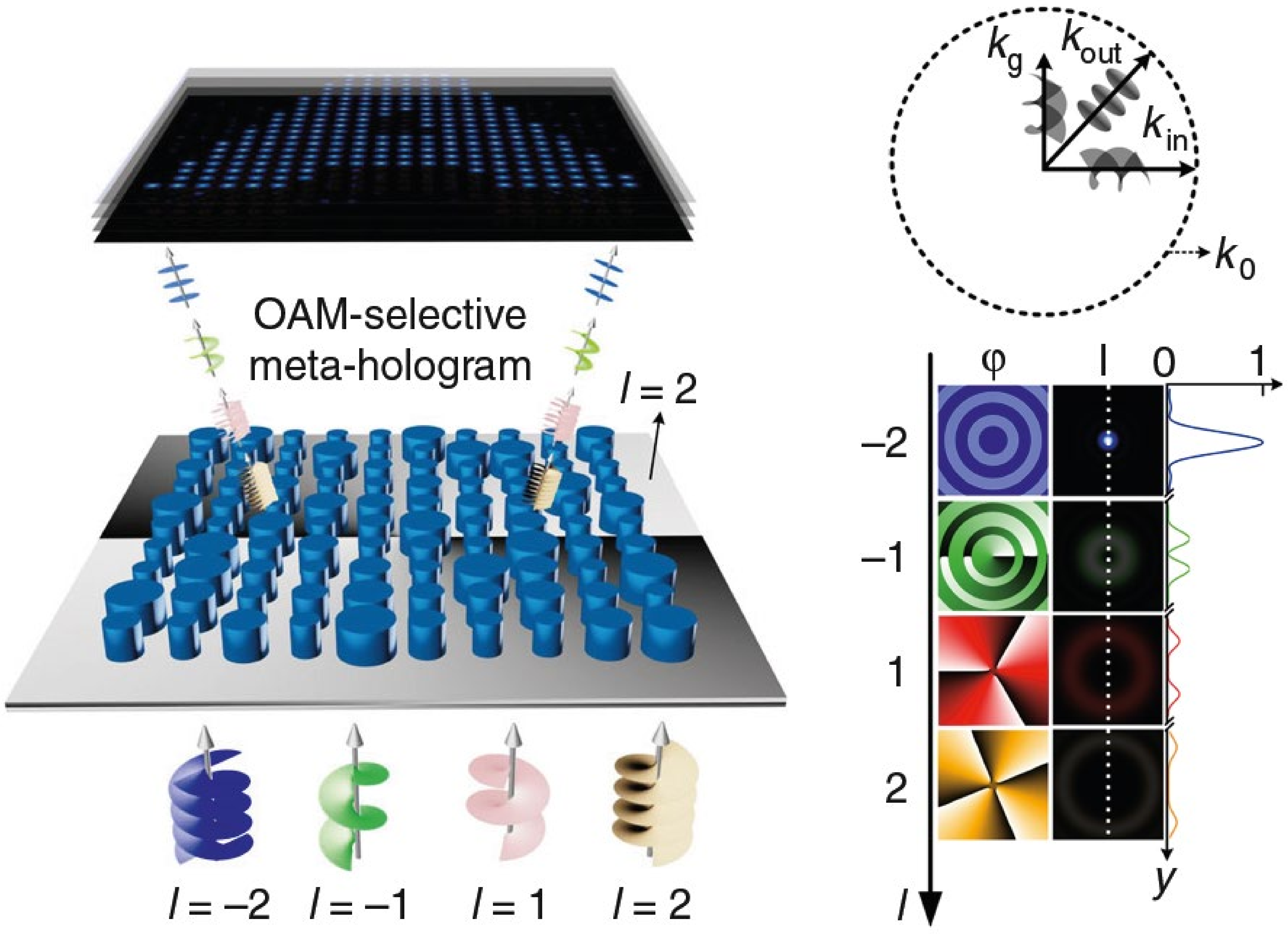

OAM-conserving hologram + spiral phase plate of phase distribution $l\varphi$ converts OAM of topological charge -*l* into fundamental mode

Phase-only OAM multiplexing holography

Nature Communications **10**, 2986 (2019)

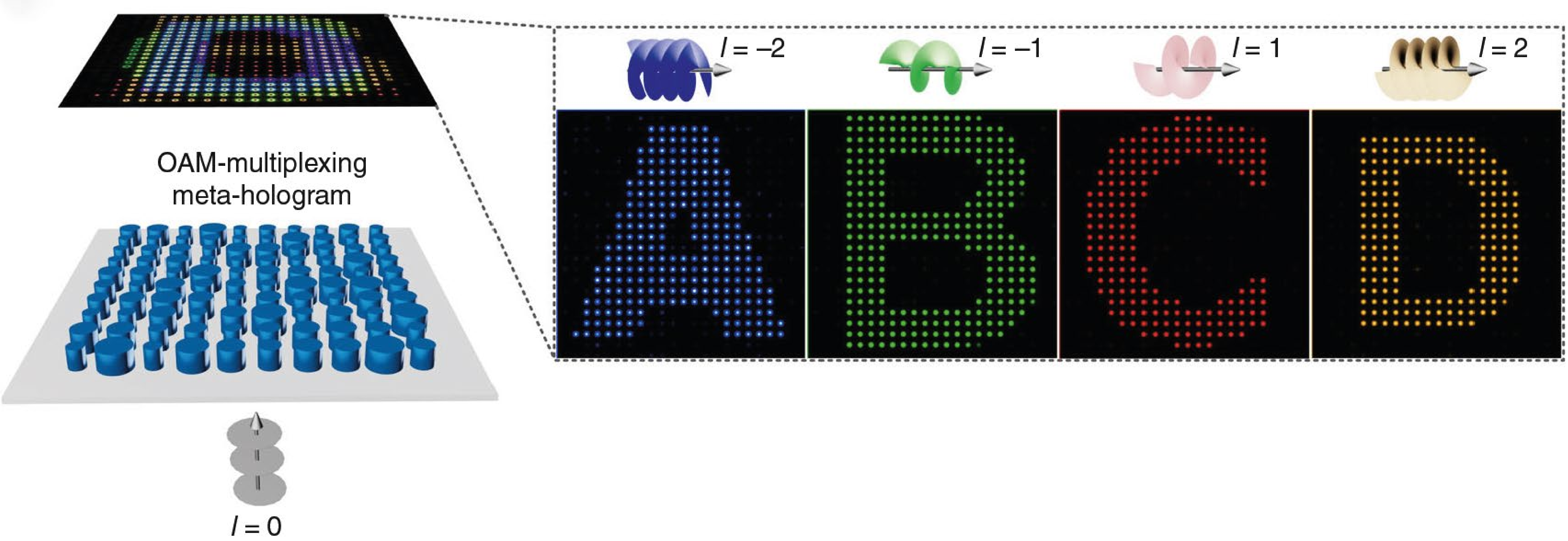

Superposition of multiple OAM-selective holograms:
Different OAM modes carry independent information channels

Lensless reconstruction of holographic images

Nature Communications **10**, 2986 (2019)

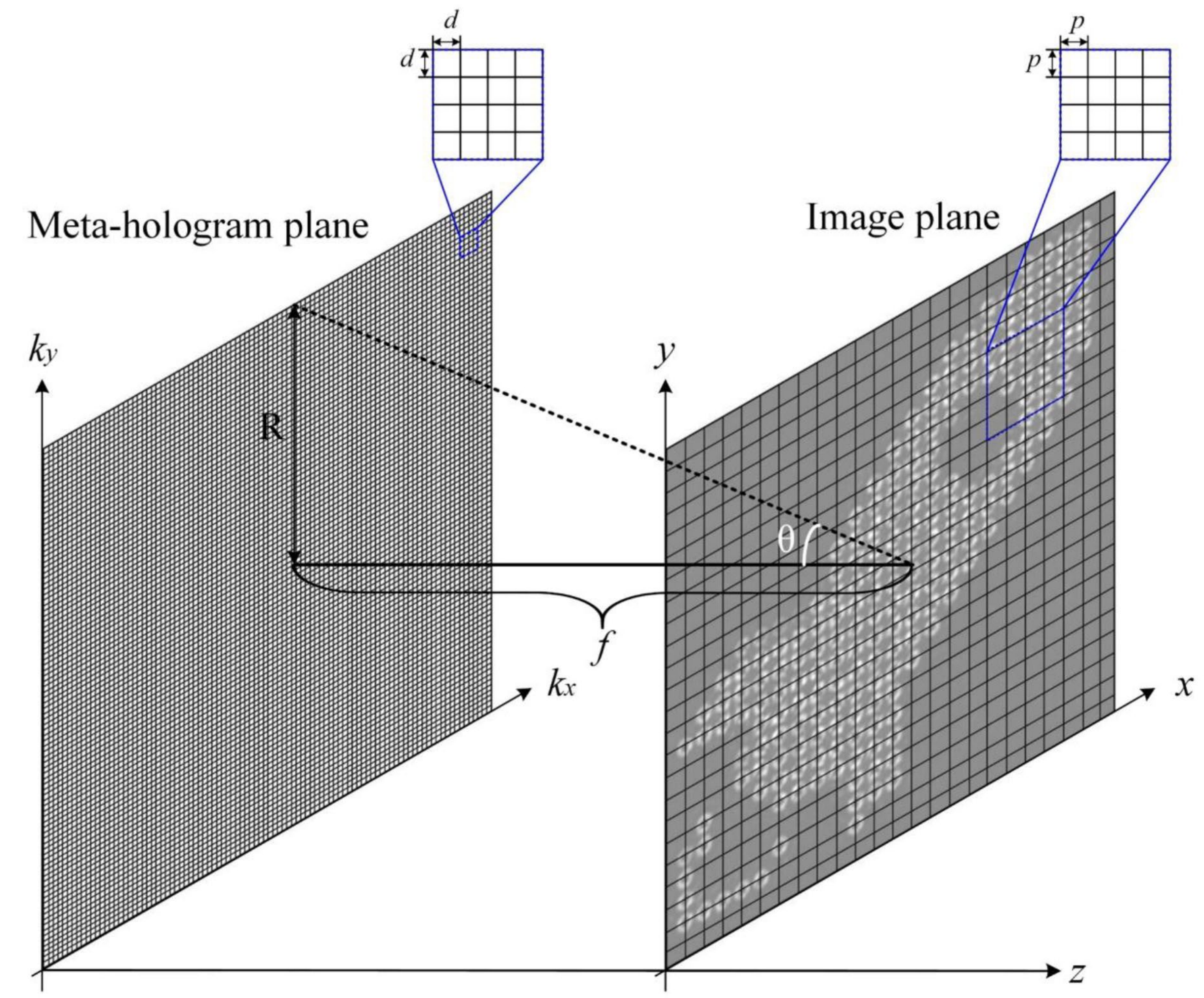

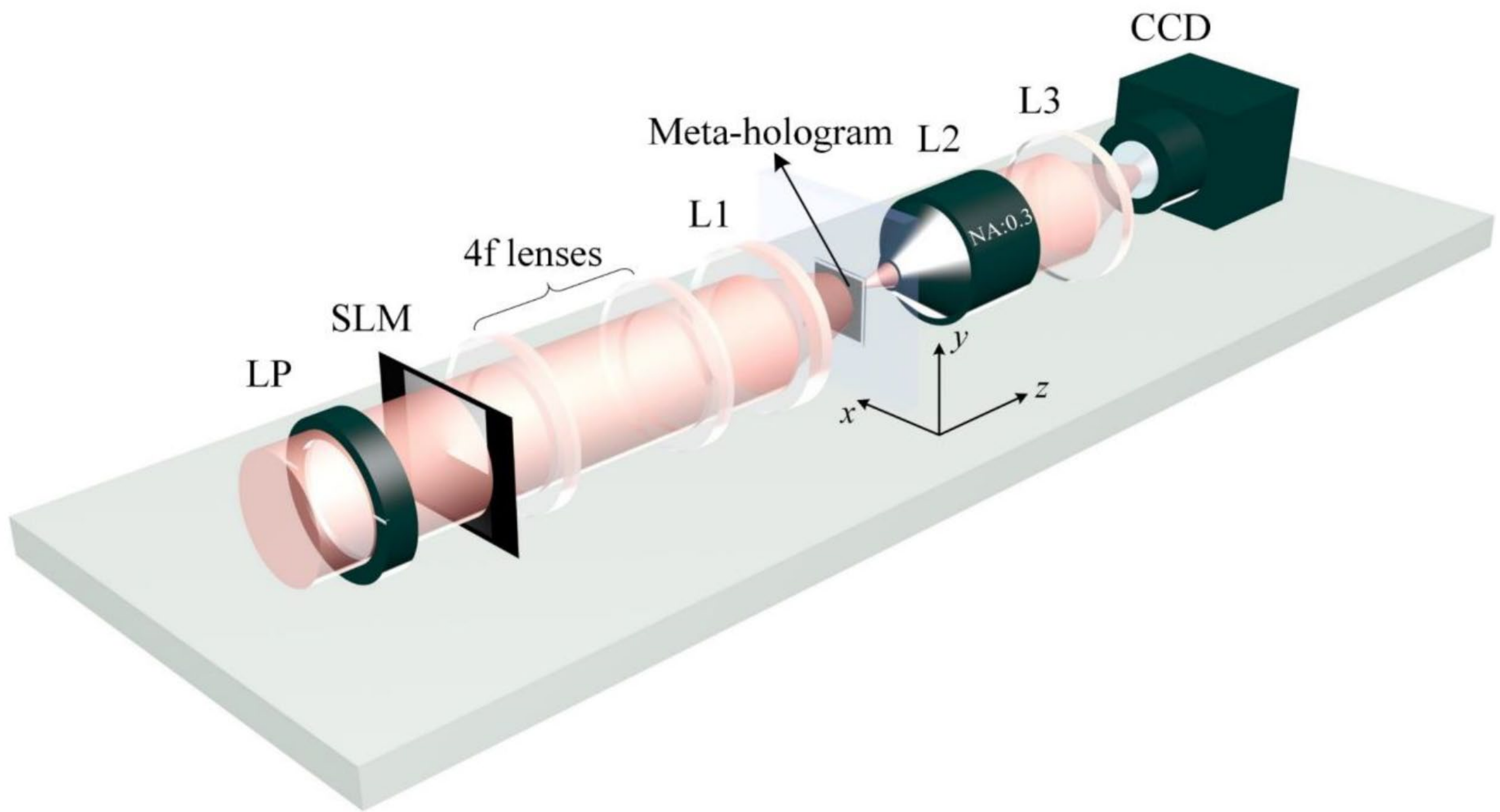

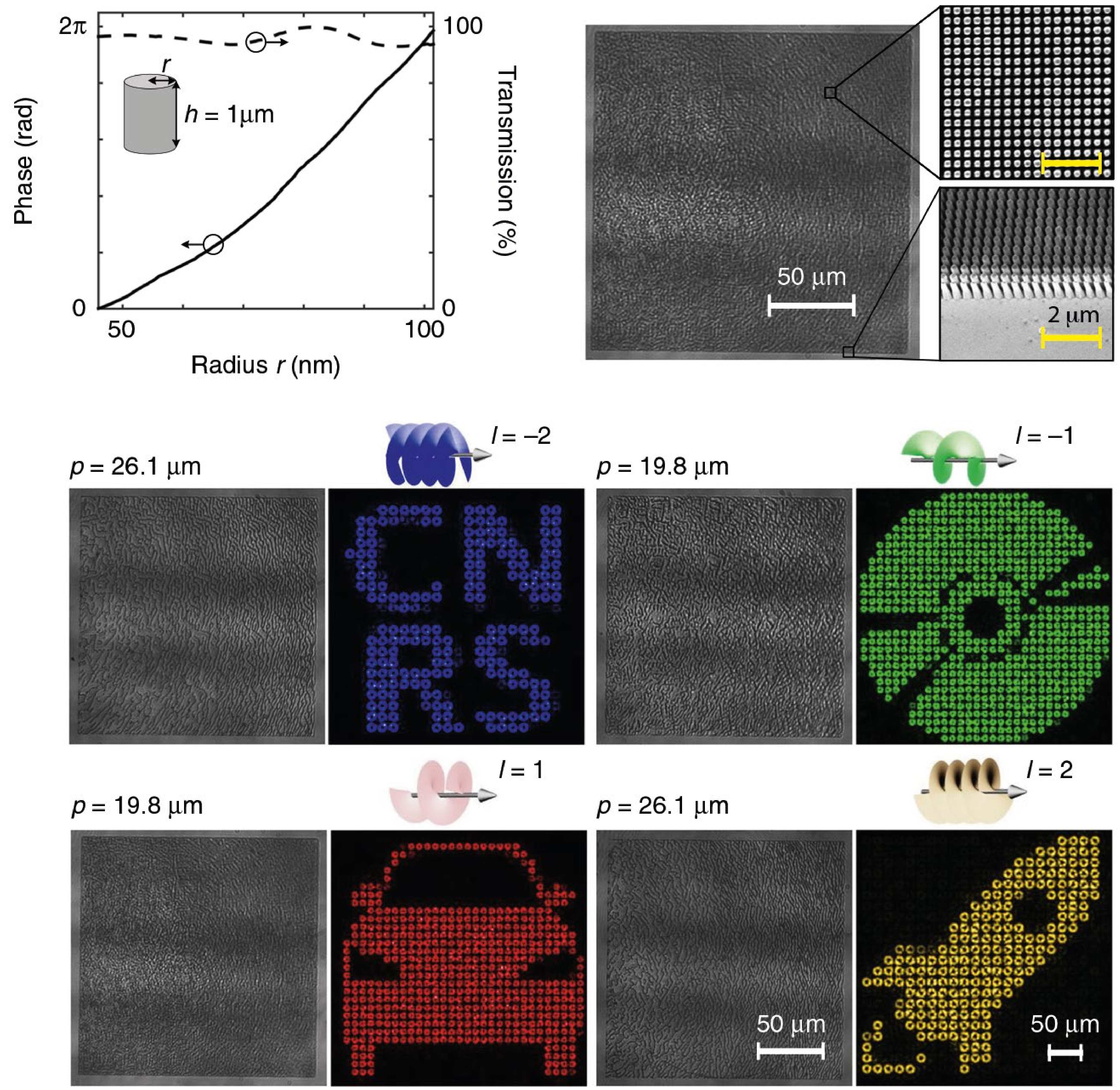

Realization of OAM-preserving holograms via GaN nanopillars of fixed height and varying radii

Selectivity and multiplexing

Nature Communications **10**, 2986 (2019)

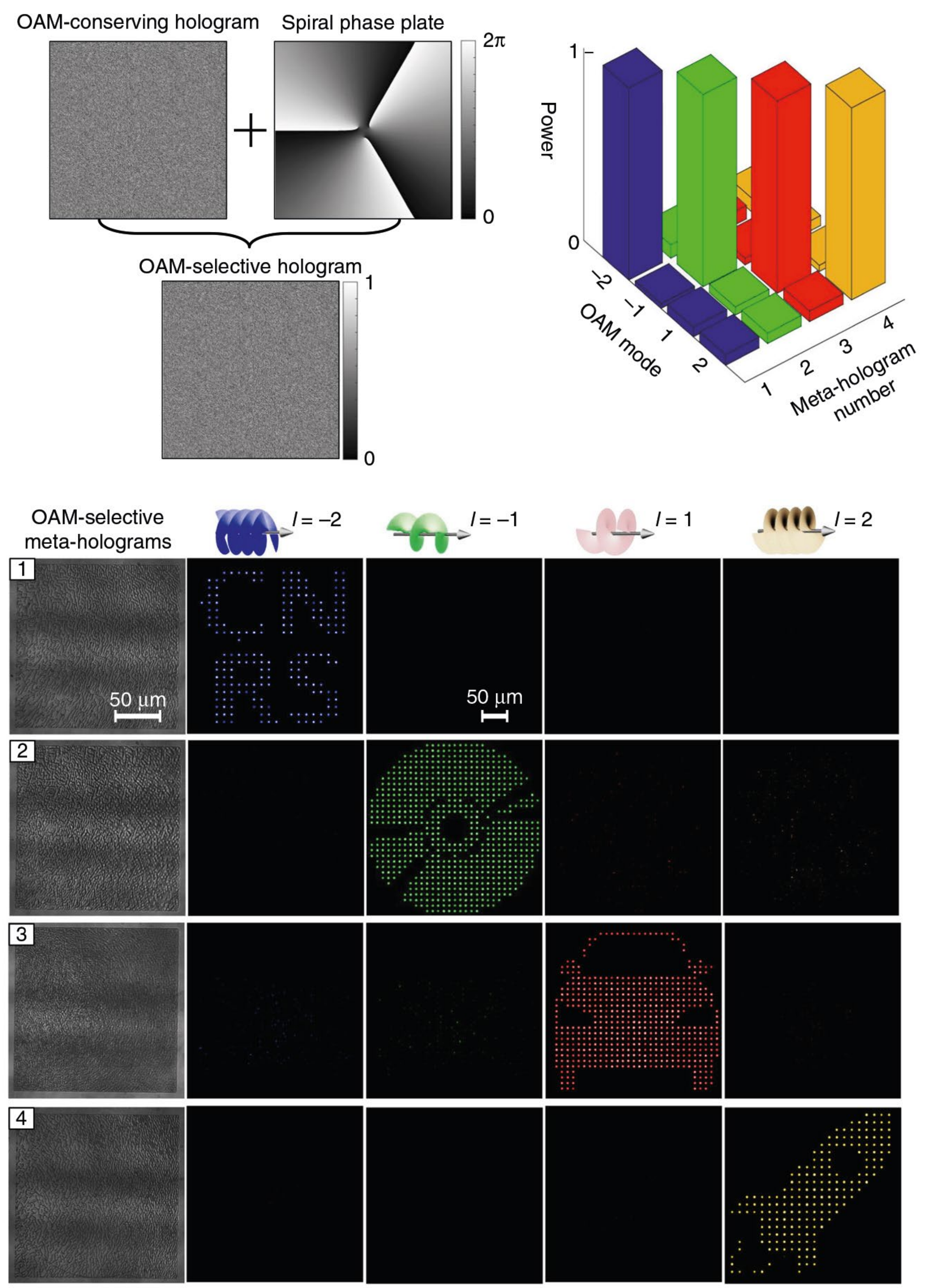

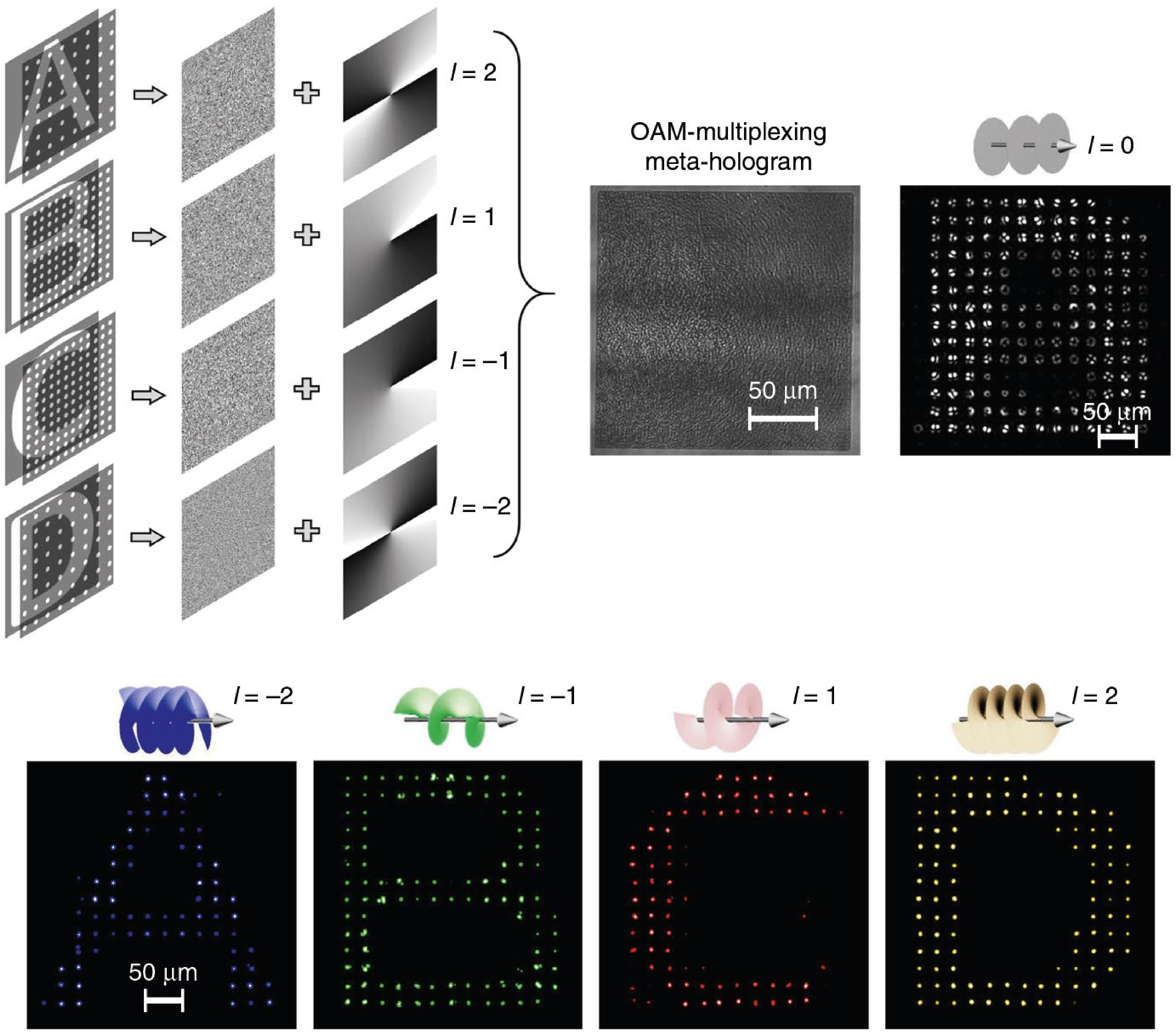

Adjustment of CCD pixel sensitivity commensurate with OAM-dependent sampling constants aids mode selectivity

Complex-amplitude metasurface holography

Nature Nanotechnology **15**, 948 (2020)

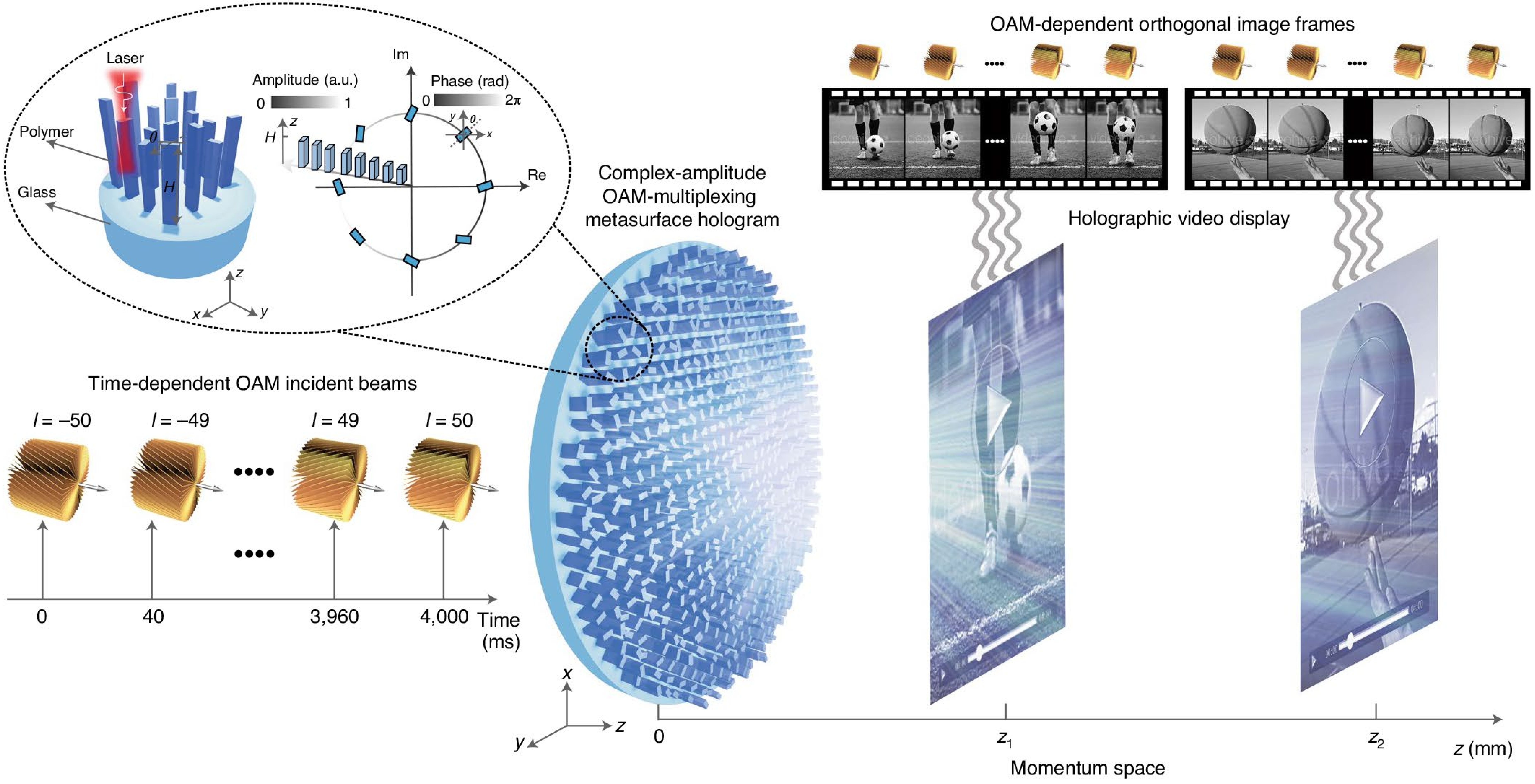

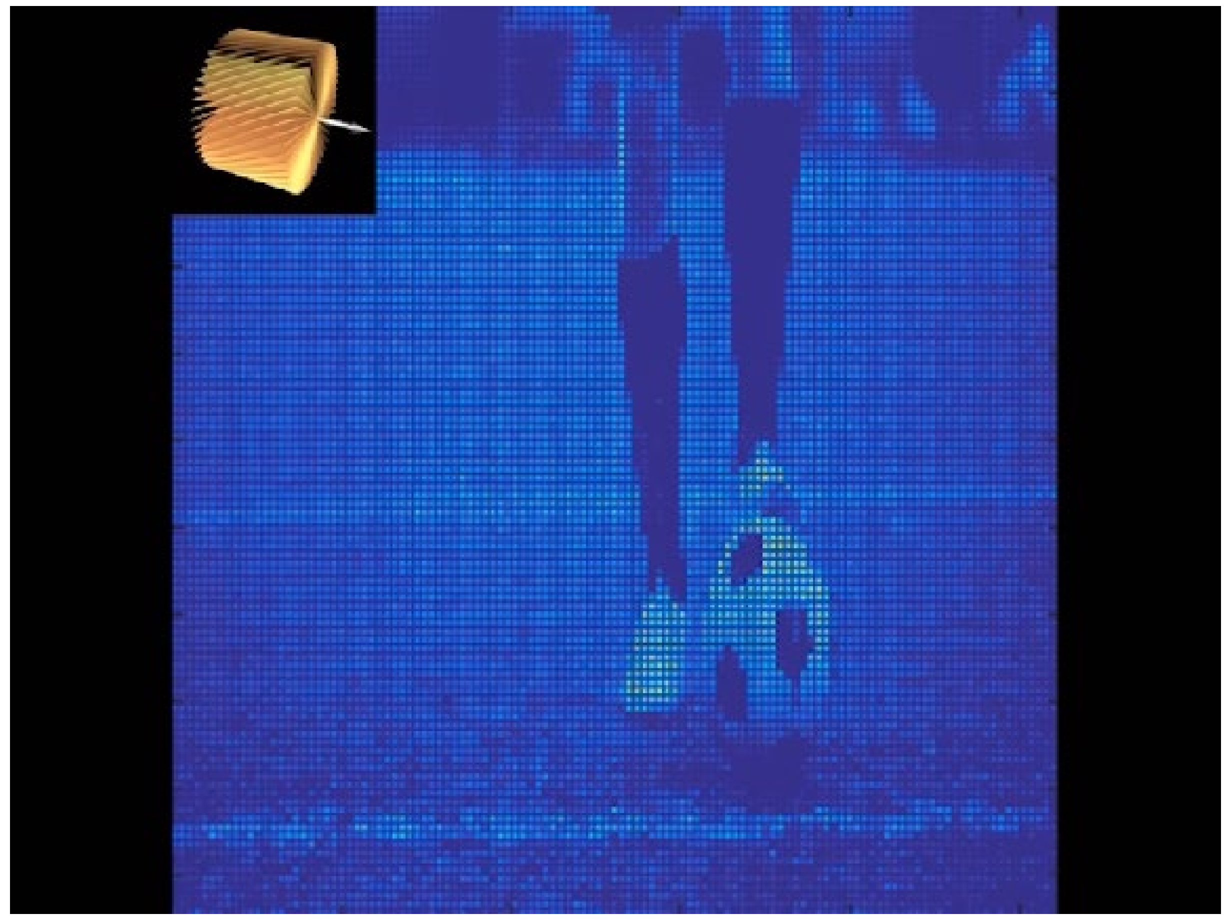

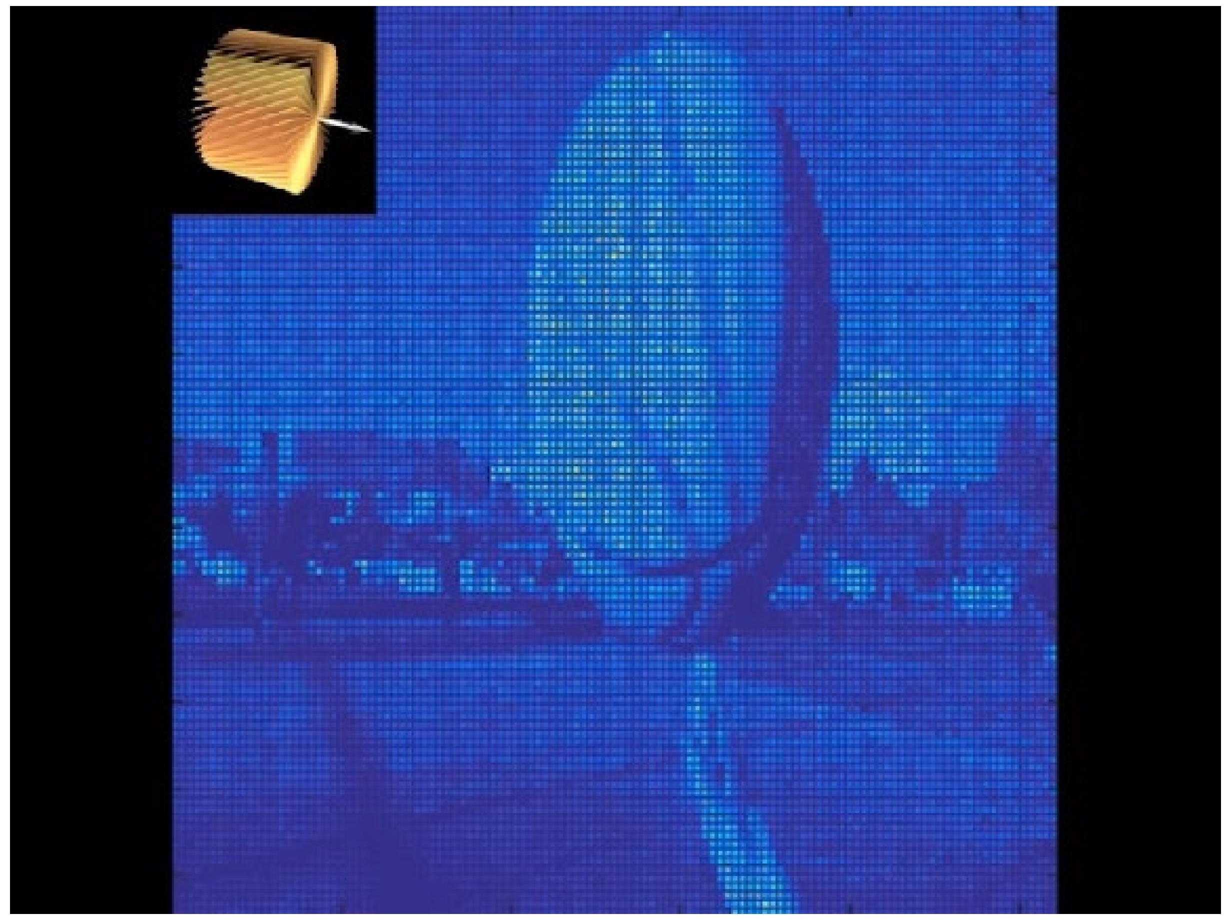

Height and in-plane rotation of birefringent polymer nanopillars allow independent control over amplitude and phase

Flowchart for holographic video encoding

Nature Nanotechnology **15**, 948 (2020)

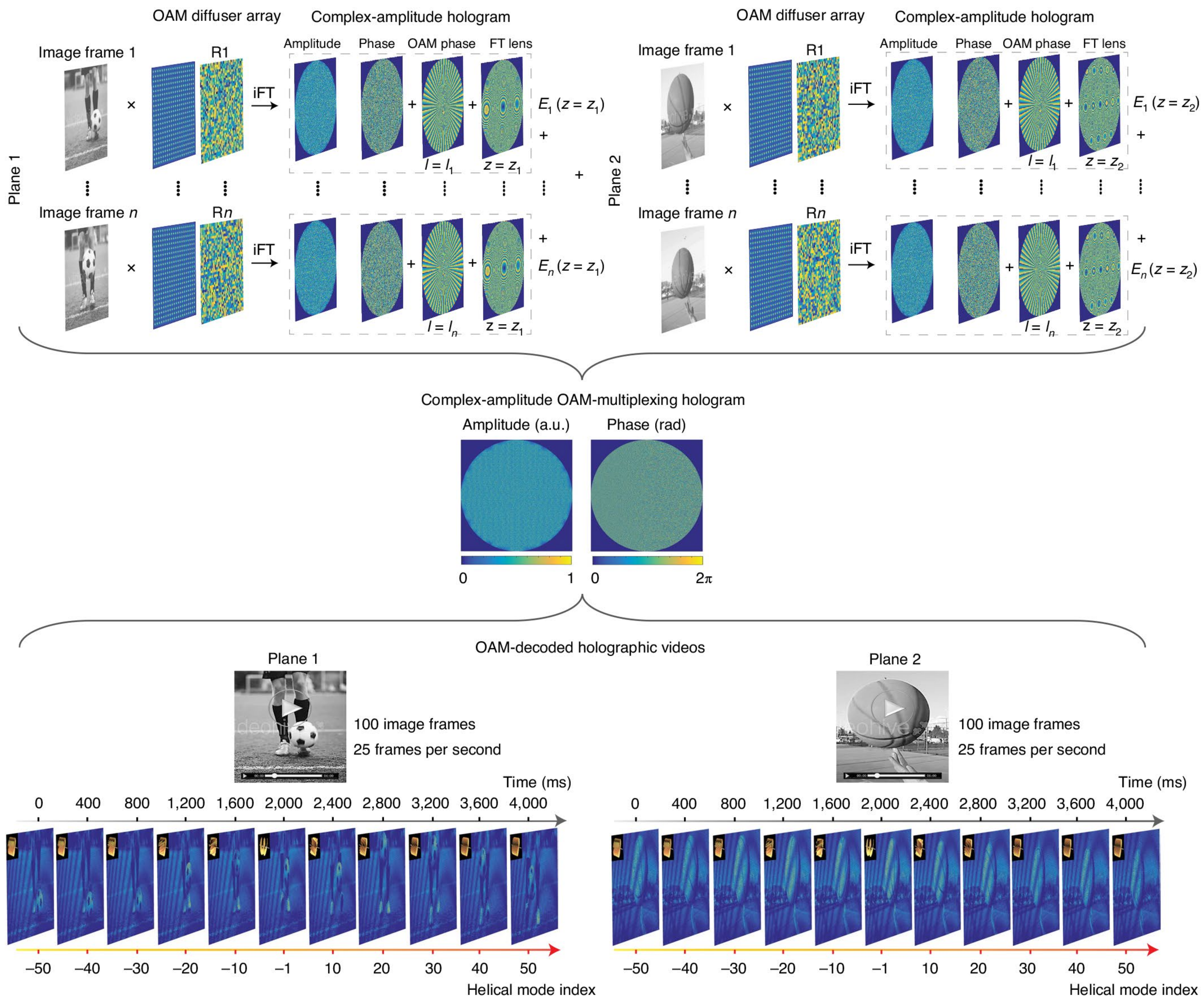

Transfer of time-sequence information to the OAM degree of freedom

Complex-amplitude modulation via polymer nanopillars

Nature Nanotechnology **15**, 948 (2020)

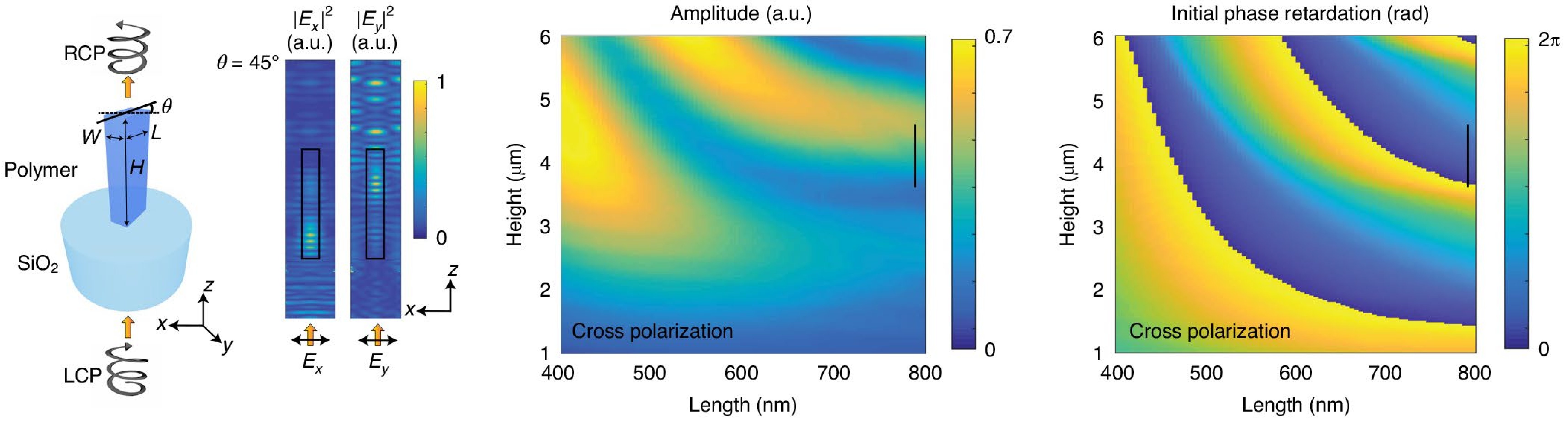

64 level complex-amplitude modulation

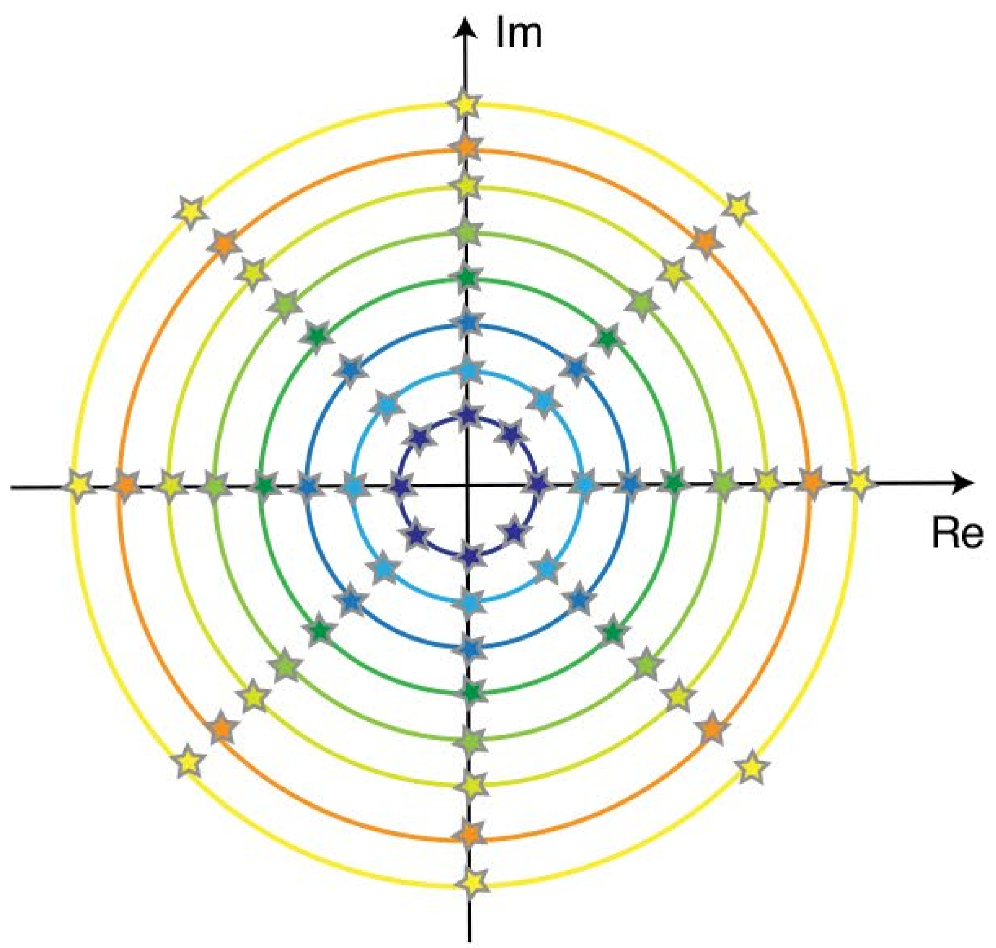

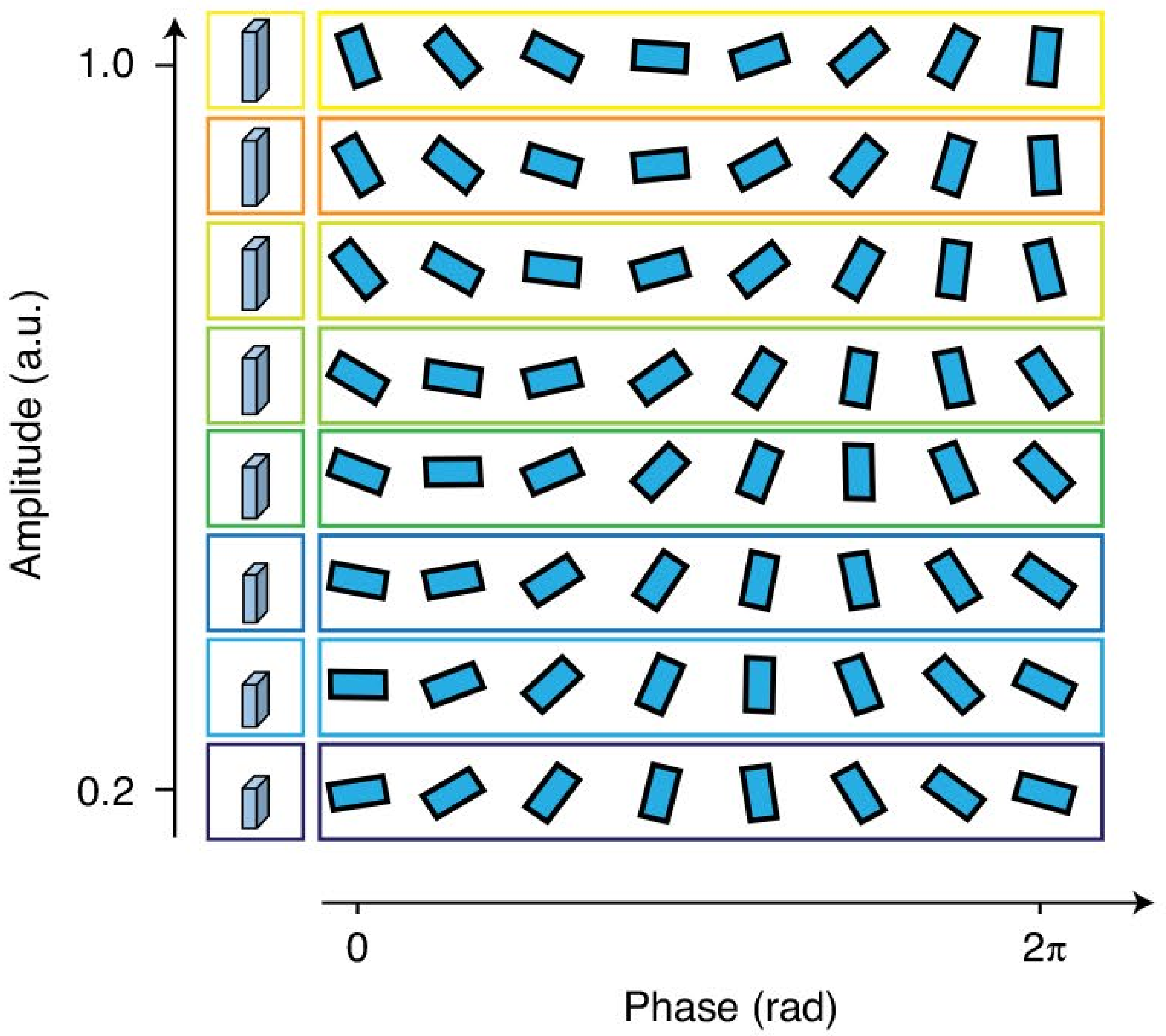

3D laser-printed complex-amplitude metasurface

Nature Nanotechnology **15**, 948 (2020)

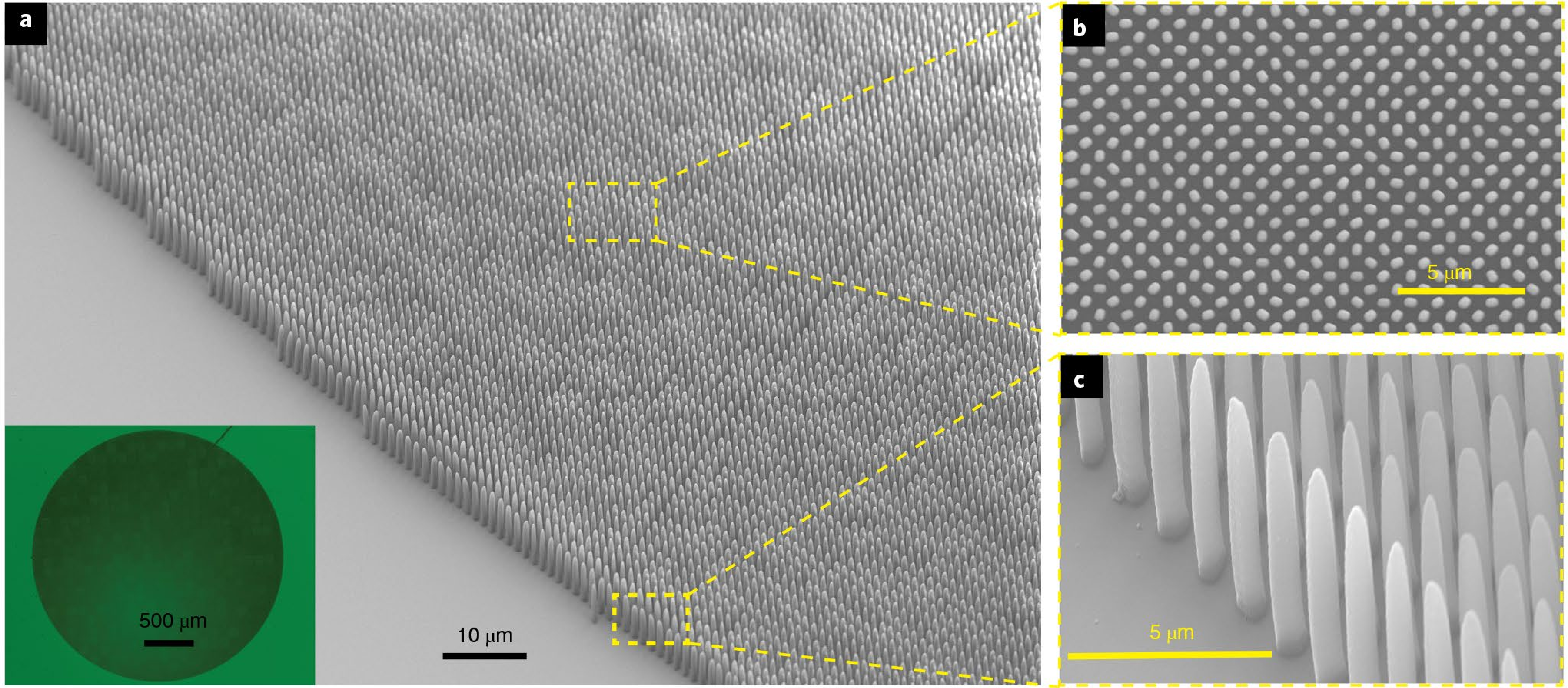

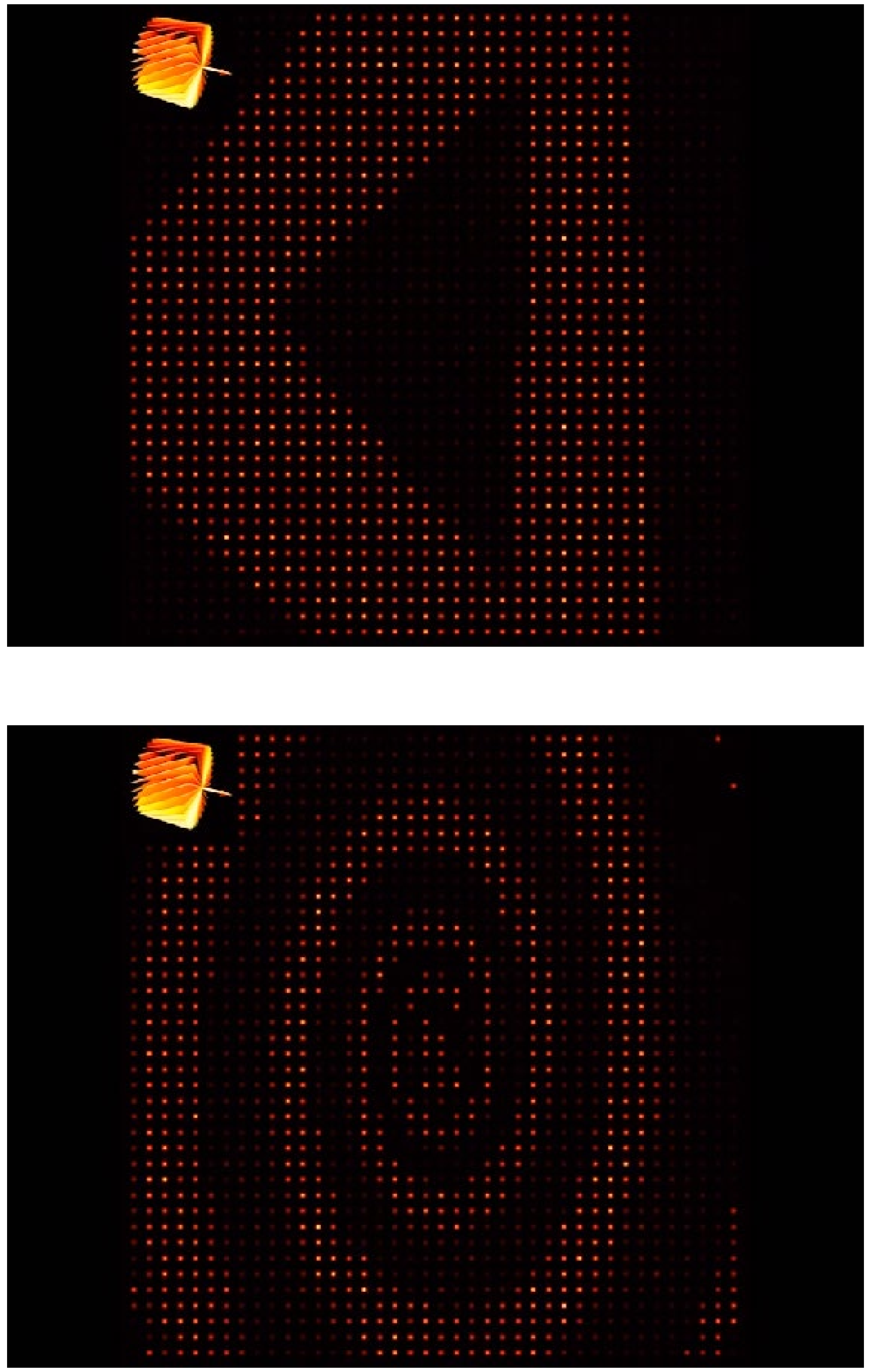

Demonstration of 2000x2000 pixels video reconstruction in two separate image planes

Application in high-security encryption

Nature Nanotechnology **15**, 948 (2020)

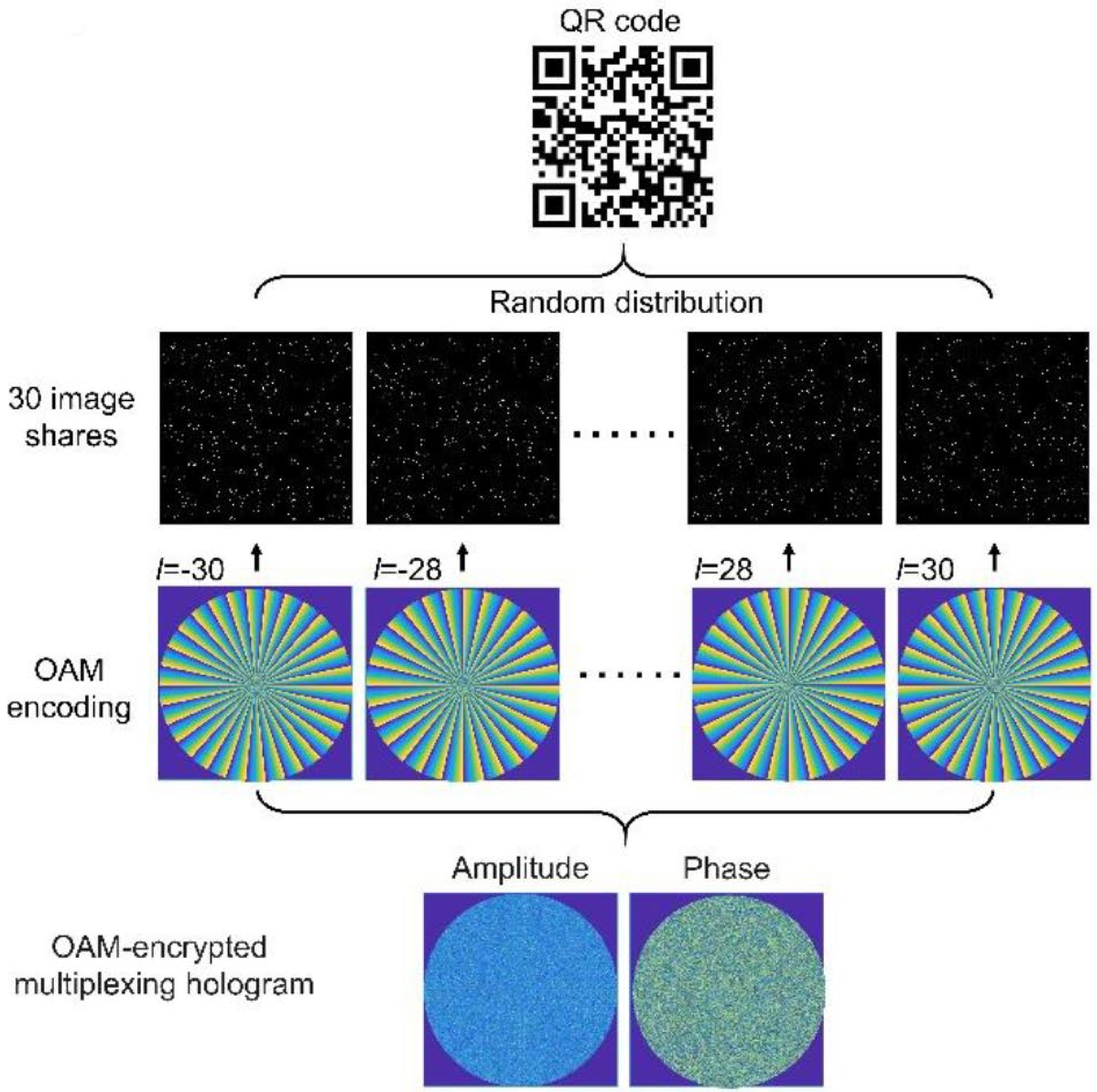

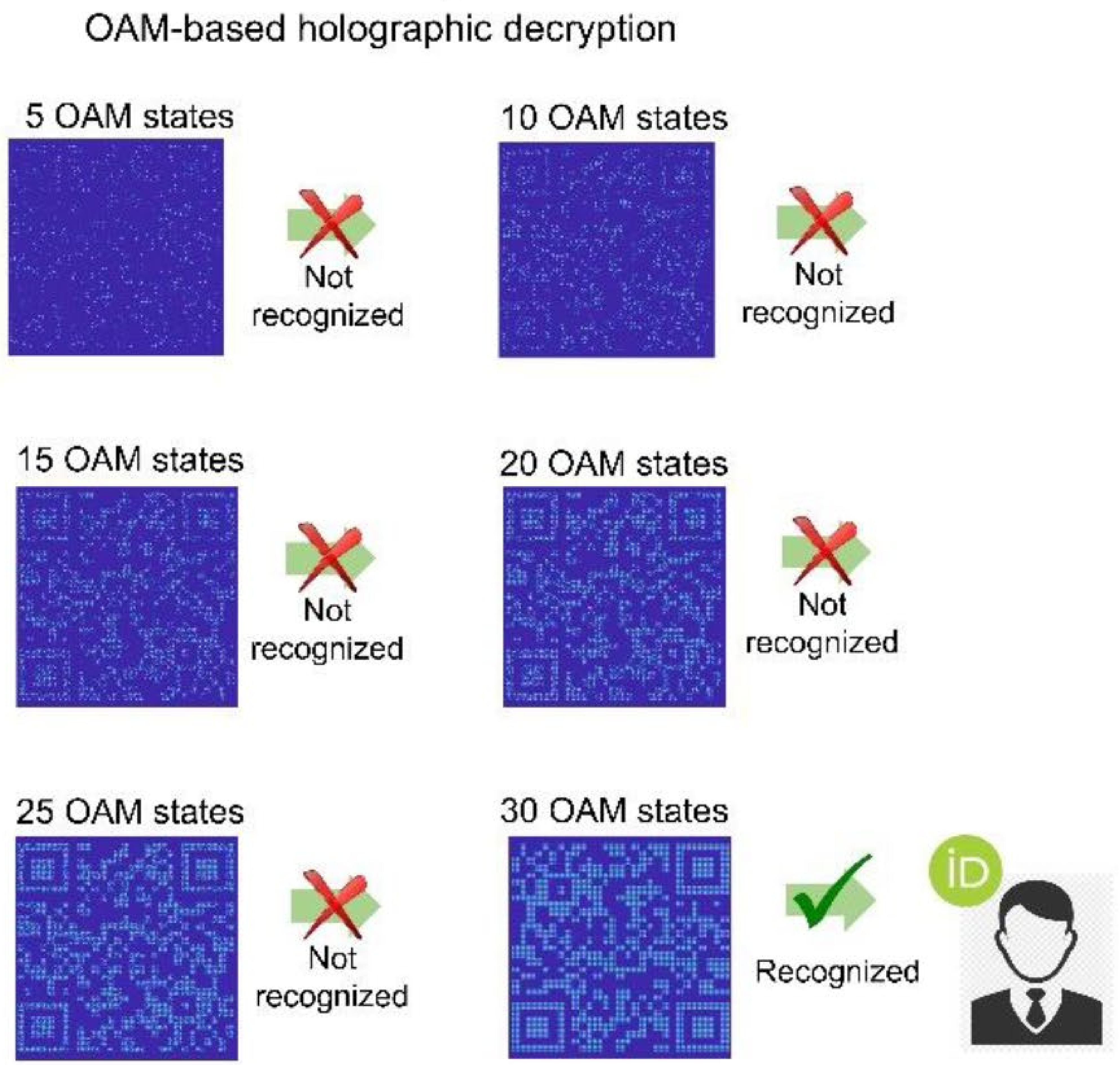

Outline

Metasurface holography

Nature Nanotechnology **15**, 948 (2020)
Nature Communications **10**, 2986 (2019)

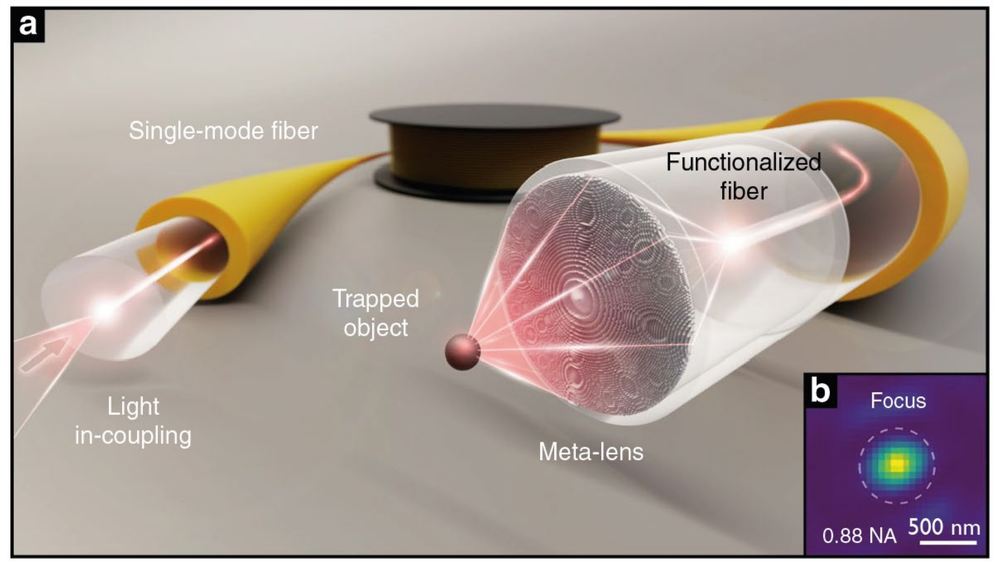

Meta-optics for optical fibre applications

*arxiv.org/abs/***2201.07158**
Light: Science & Applications **10:57** (2021)

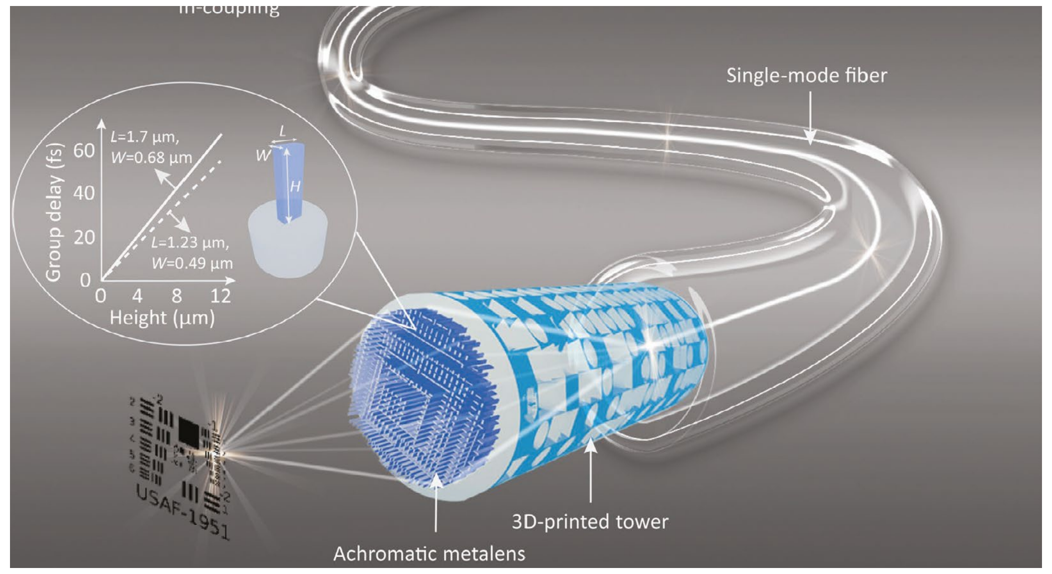

Complex-amplitude metasurfaces for fiber optics

*arxiv.org/abs/*2201.07158

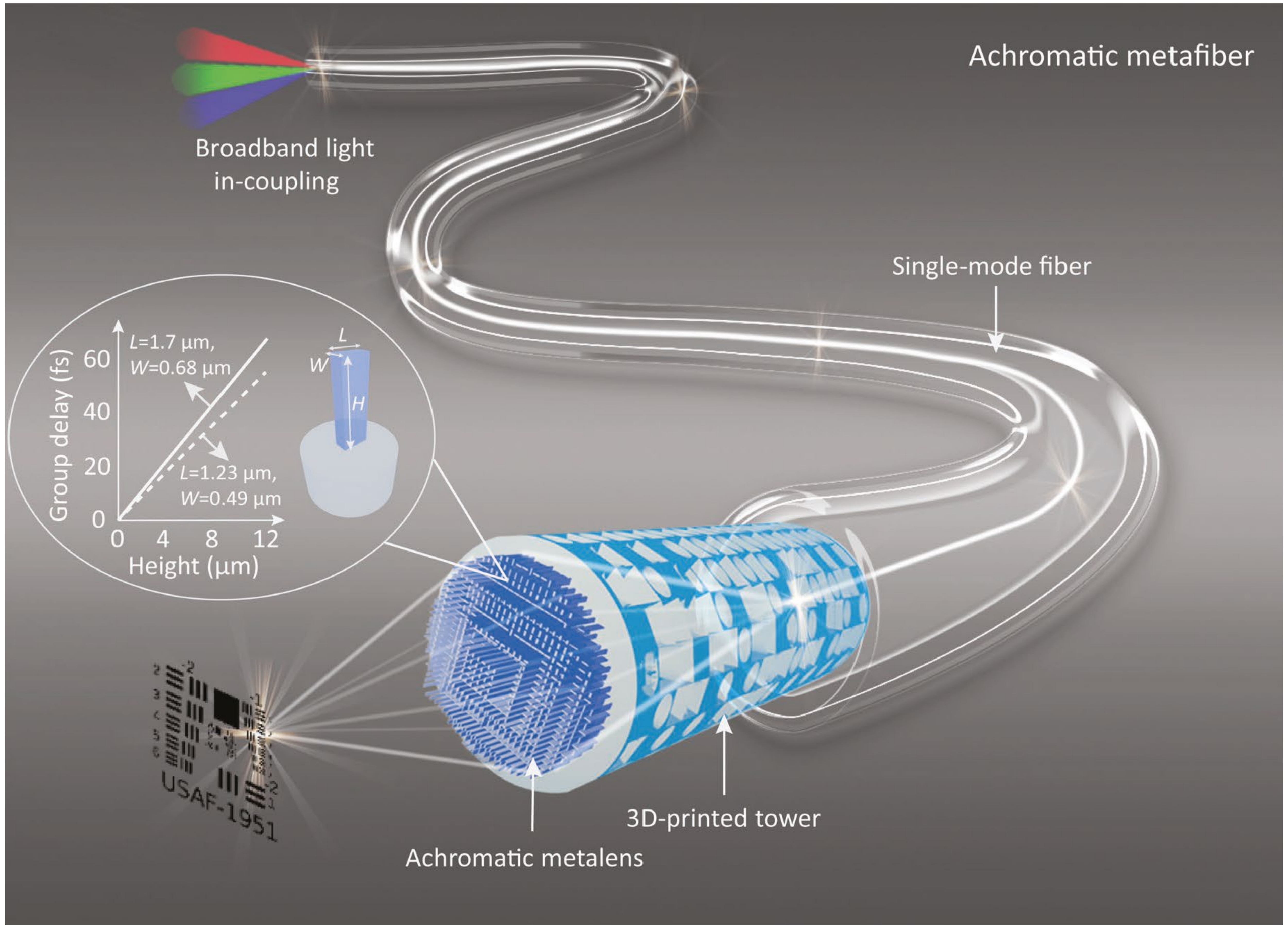

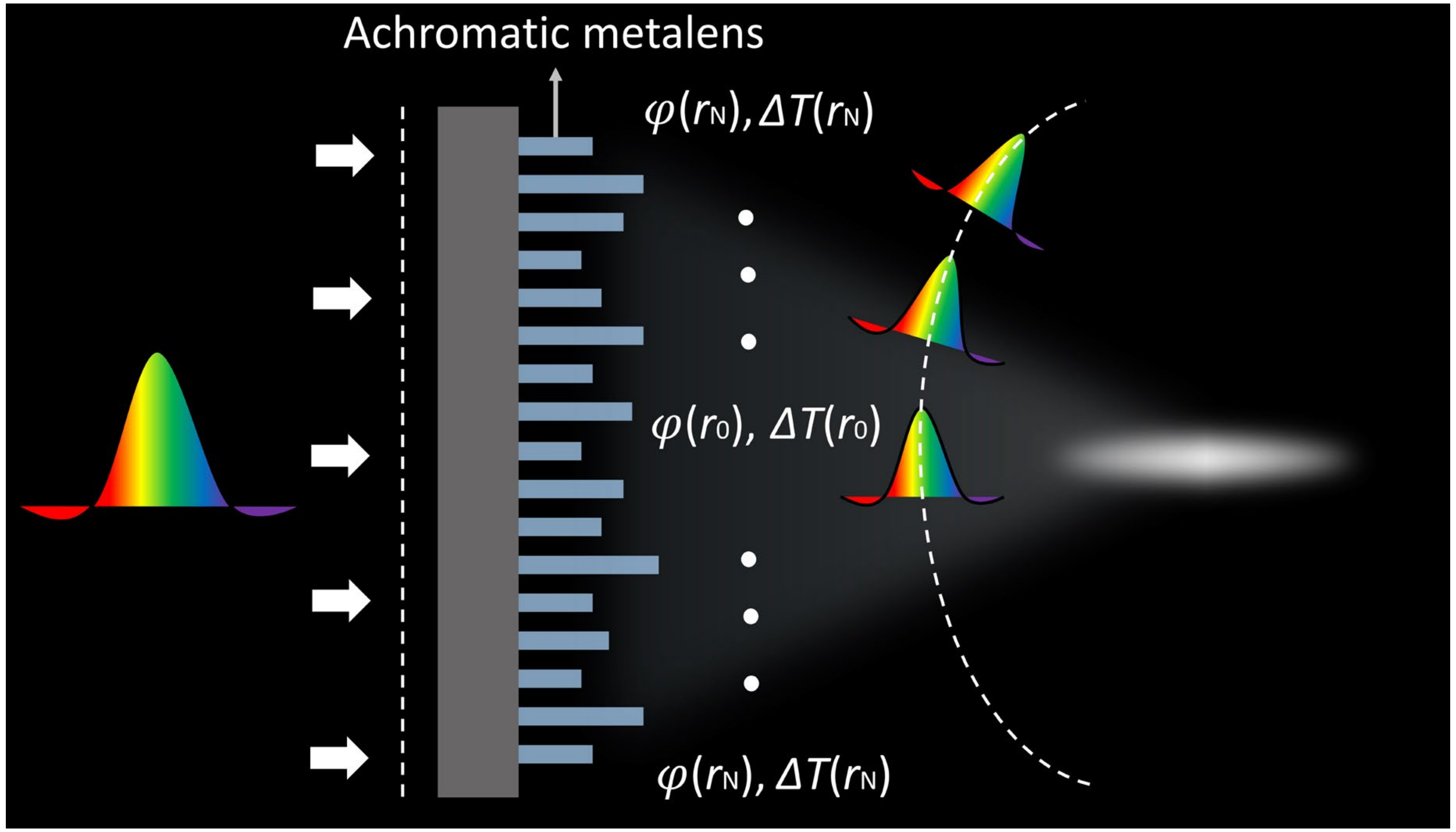

Design of an achromatic metalens for the telecommunication range:
radially arranged phase profile for focusing and group delay profile for arrival time compensation

Achromatic focusing and broadband imaging

*arxiv.org/abs/***2201.07158**

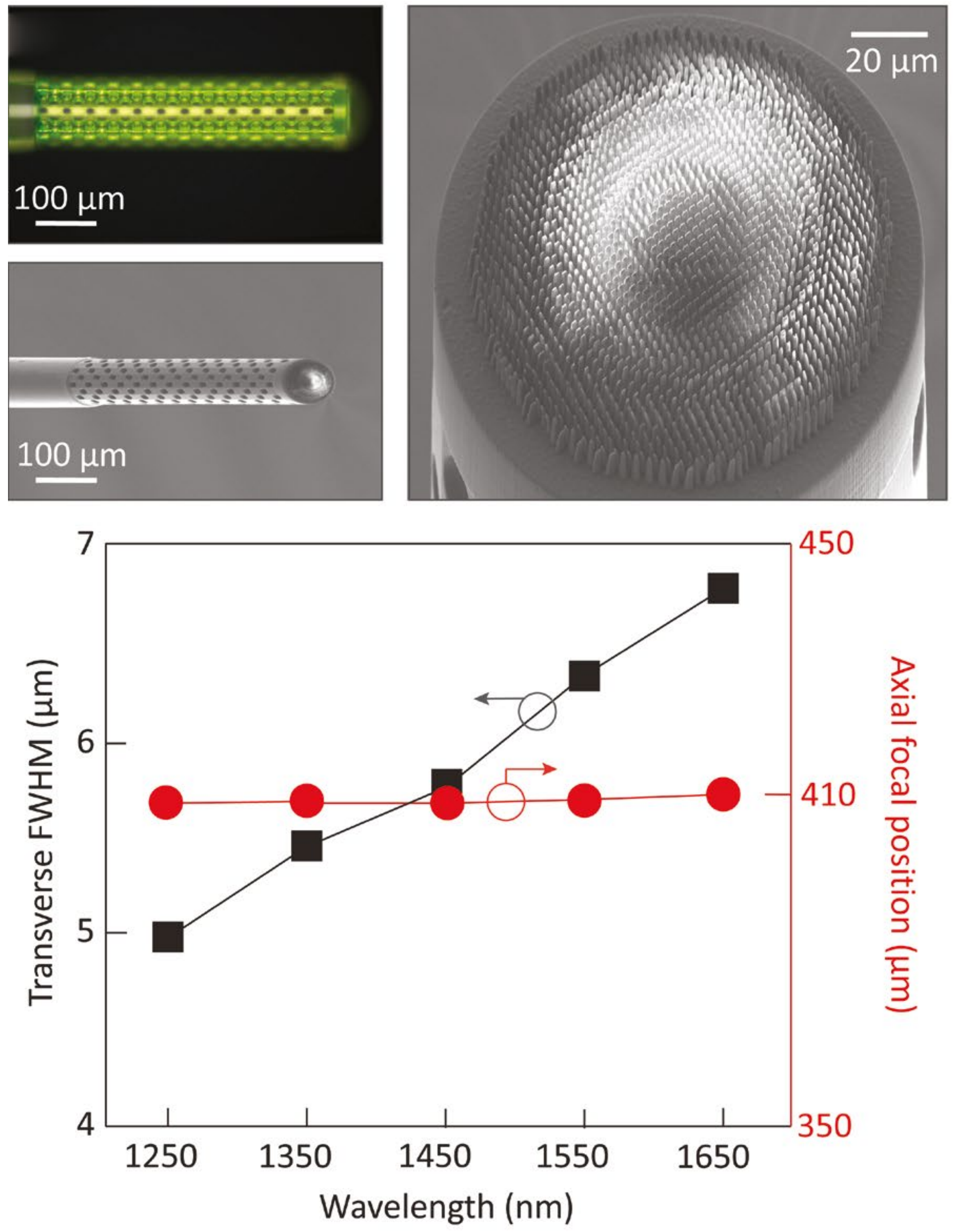

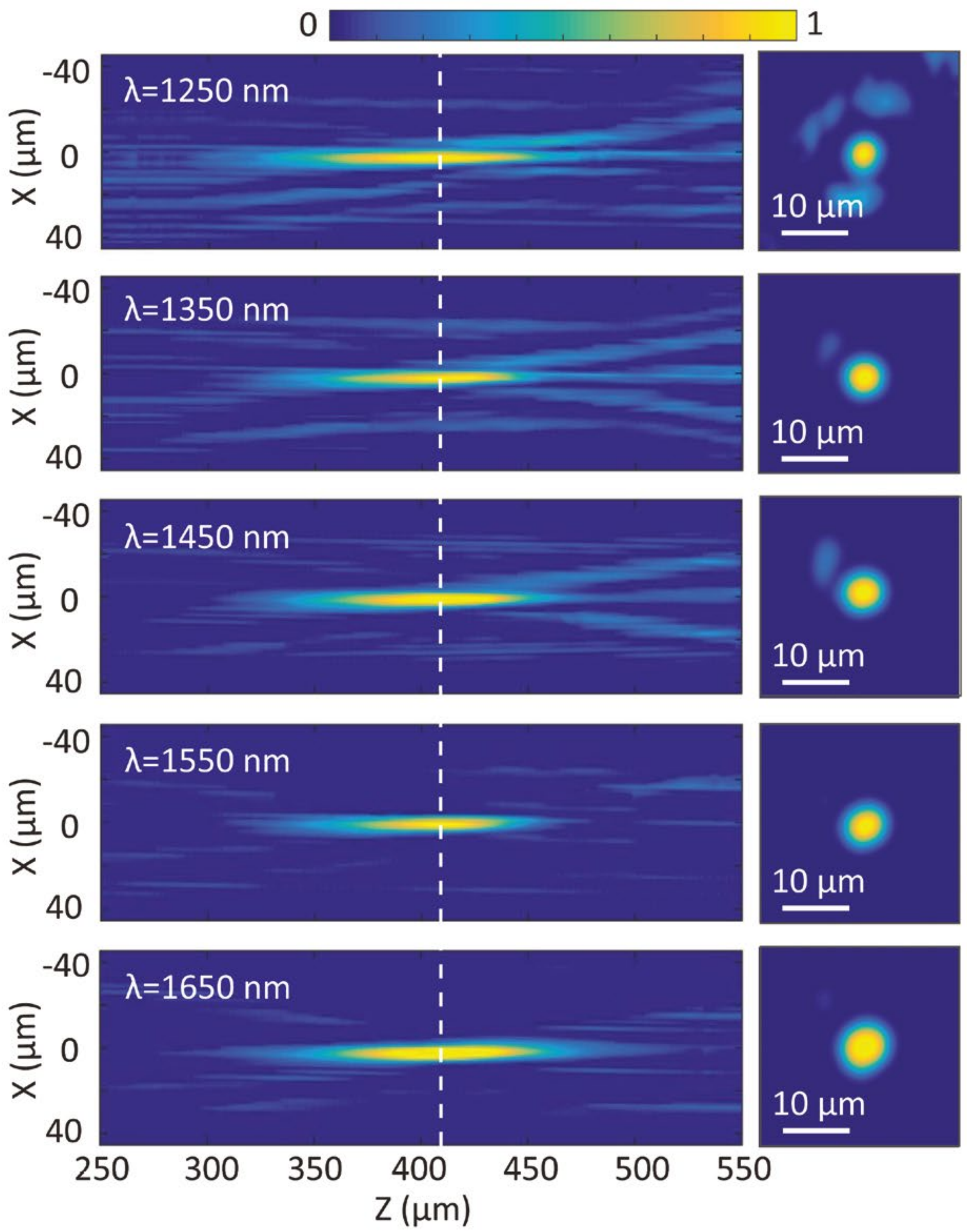

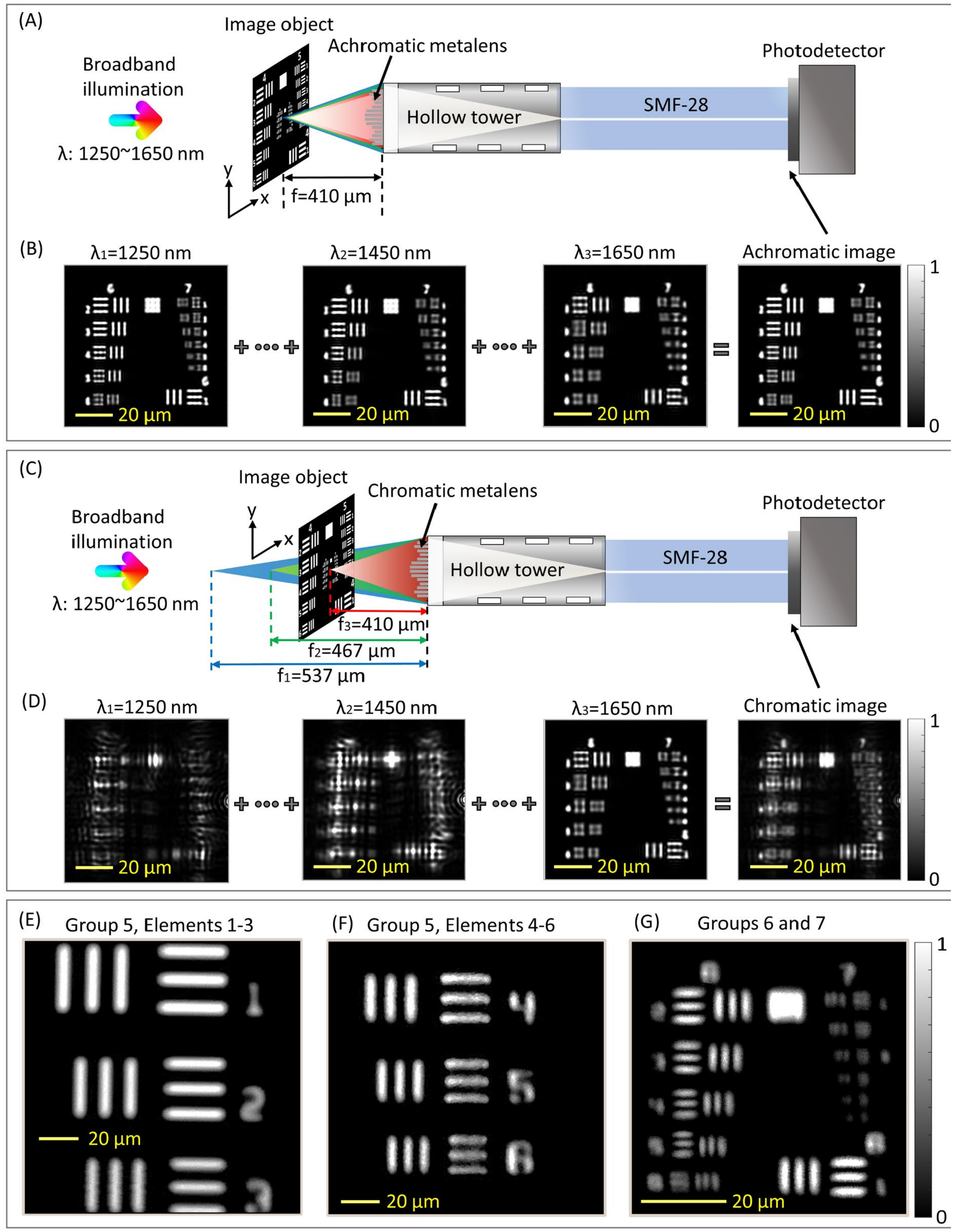

Record bandwidth of 400 nm over the whole telecommunications range

Ultrahigh numerical aperture meta-fibre for trapping

Light: Science & Applications **10:57** (2021)

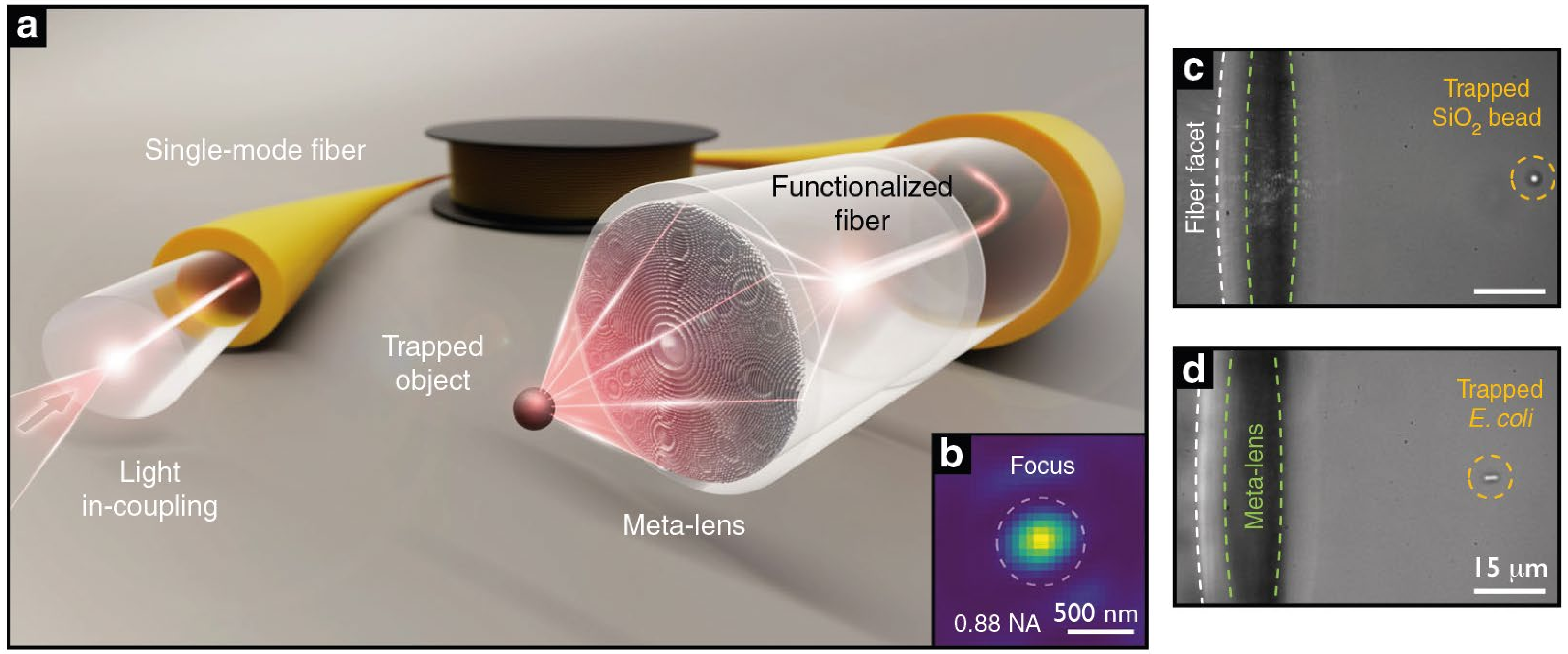

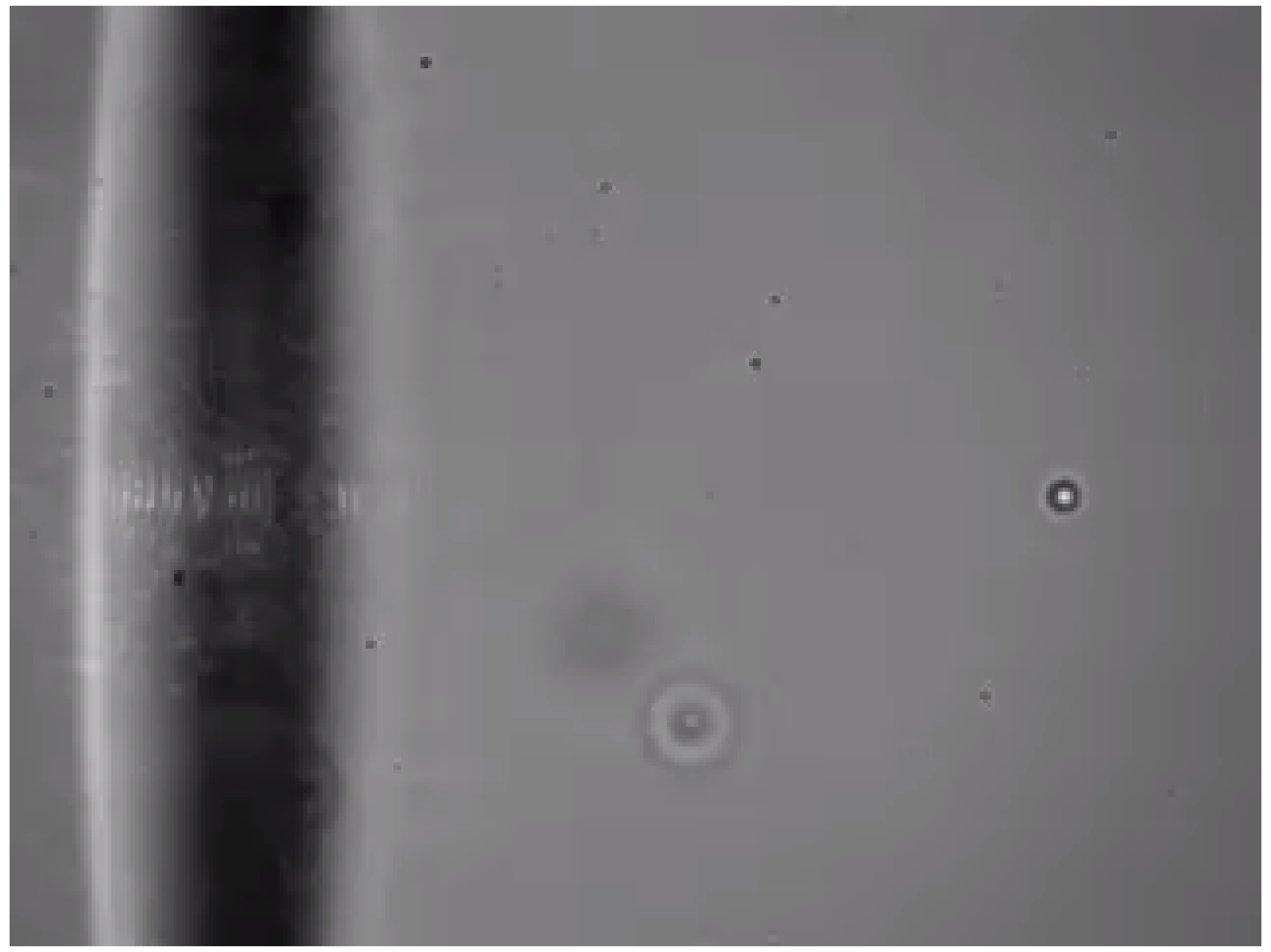

2 µm silica sphere

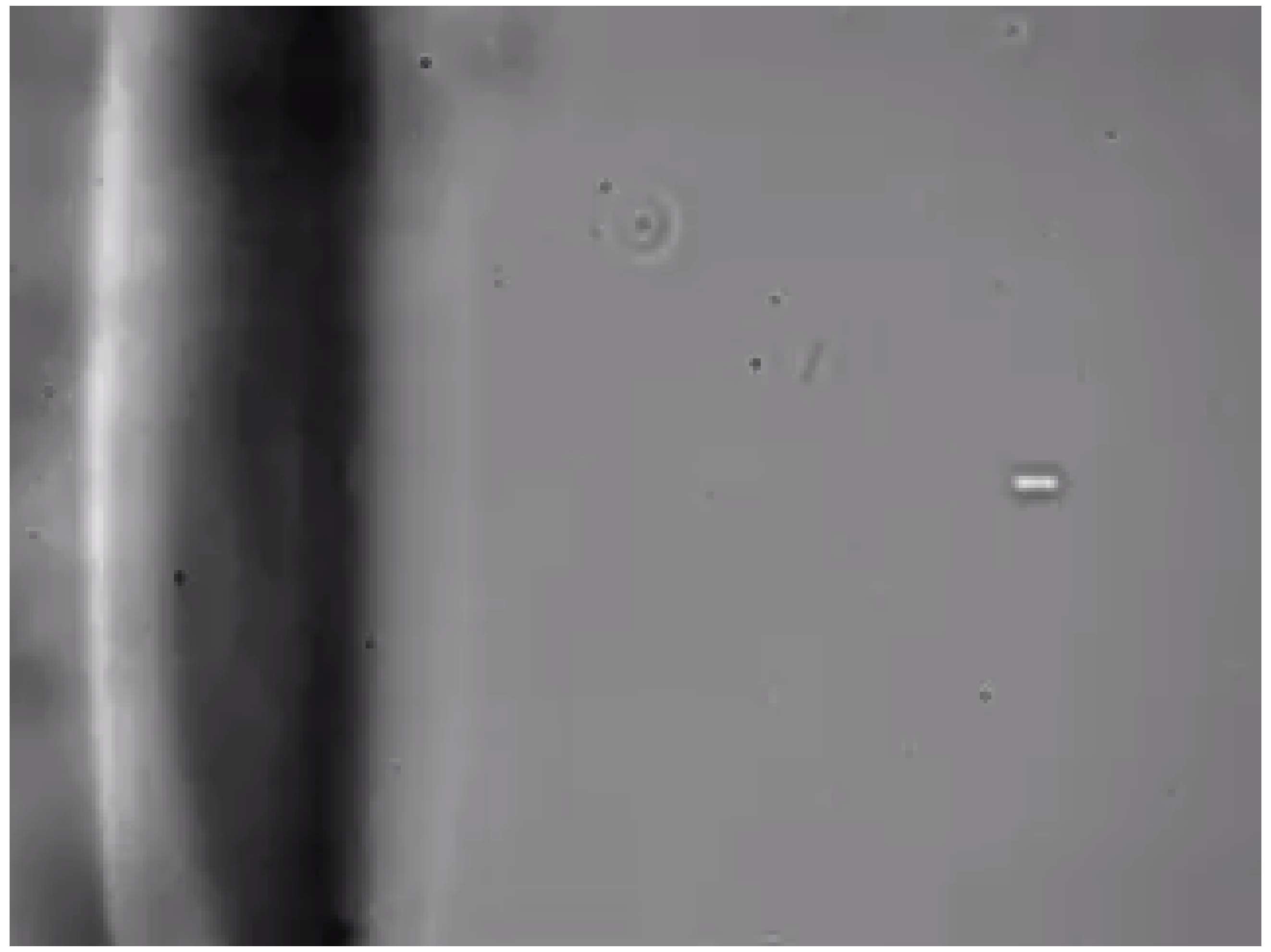

E. coli bacterium

Focusing and trapping in context

Light: Science & Applications **10:57** (2021)

Working principle	Fabrication method	Lens material	Fibre type	Wavelength	Measured NA	Trapping application	Reference
Refractive microprism	Two-photon lithography	Polymer	4 SMF bundle	1070 nm	1.15 water (theor.)	Red blood/ tumour cells	ref. [51]
Diffractive meta-lens	fs direct laser writing	Polymer	1 SMF + MMF spliced	660 nm	0.882 water	2 μm beads/ E. coli	This work
Refractive ball lens	Glue	SiO_2	1 SMF + MMF spliced	980 nm	0.875 water	0.2 μm beads/ yeast cells	ref. [52,53]
Digital holography	Spatial light modulator	–	1 MMF	1064 nm	>0.8 water	1.5 μm beads	ref. [14]
Diffractive meta-lens	fs direct laser writing	Polymer	2 SMFs + spacer printed	808 nm	0.7 water	1 μm/ 0.5 μm beads	ref. [22]
Plasmonic nanorods	Focused ion beam milling	Au	1 PCF	1550 nm	0.37 air	–	ref. [18]
Refractive GRIN lens	Stack & draw + glue	SiO_2	1 SMF + spacer glued	976 nm	0.16 air	2 μm beads (on the surface)	ref. [54]
Refractive microlens	Laser exposure	Polymer	1 SMF + MMF spliced	980 nm	?	8 μm beads/ yeast cells (on the surface)	ref. [55]
Diffractive Fresnel plate	Focused ion beam milling	SiO_2	1 SMF + MMF spliced	980 nm	?	8 μm beads/ yeast cells (on the surface)	ref. [17]
Diffractive Fresnel plate	UV-nanoimprint lithography	Polymer	1 SMF	660 nm	?	–	ref. [30]
Refractive microaxicon	HF chemical etching	SiO_2	1 SMF	633 nm	?	–	ref. [19]

No trapping with single fibres alone due to low NA
(additional surfaces required to overcome axial scattering force)

Design of a trapping metafibre

Light: Science & Applications **10:57** (2021)

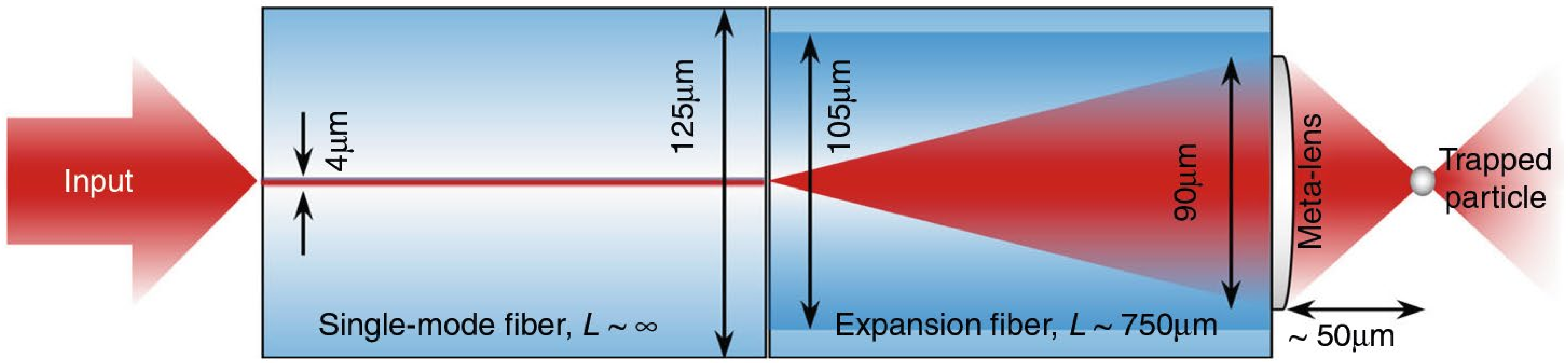

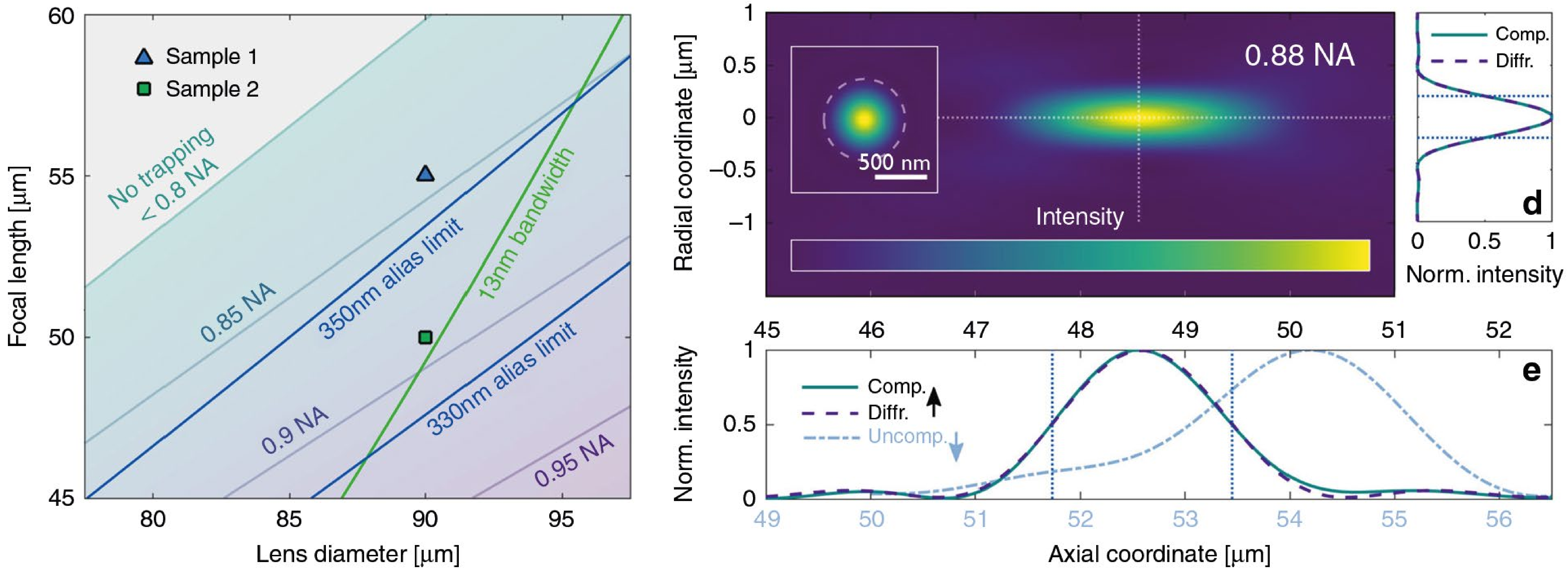

- diverging light from fibre end facet is compensated via metalens with discretized hyperbolic phase profile (kinoform-type phase distribution, circular grating diffracting at Bragg angle)
- additional compensation of curved wave fronts (spherical aberration)
- limitations: aliasing (discretization sets upper bound on achievable phase change between pixels), coherence of laser source
- resolution constraints of direct laser writing (300 nm) still enable diffraction-limited focusing with NA ≈ 0.9 at wavelength 660 nm

Implementation via direct laser writing

Light: Science & Applications **10:57** (2021)

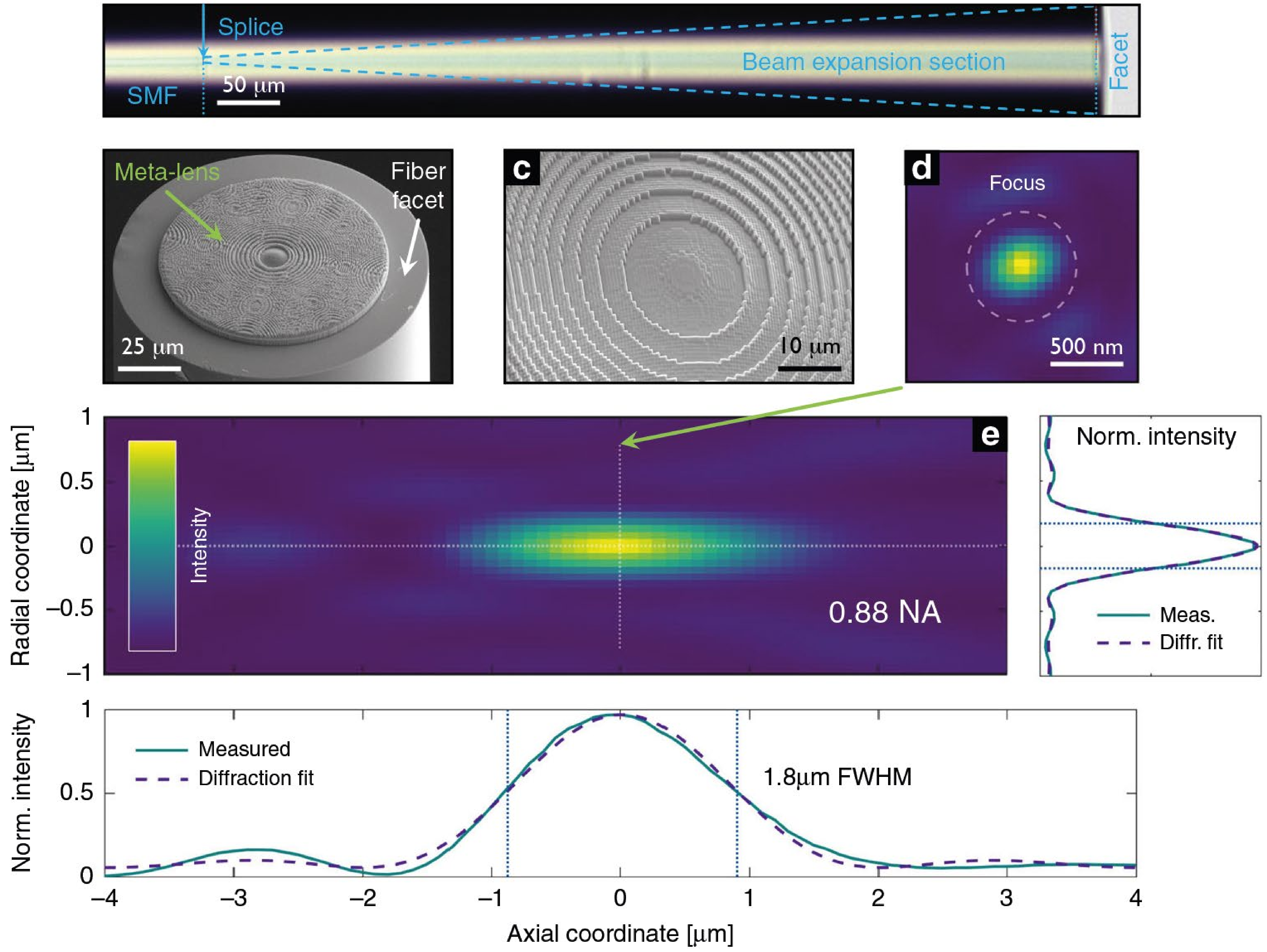

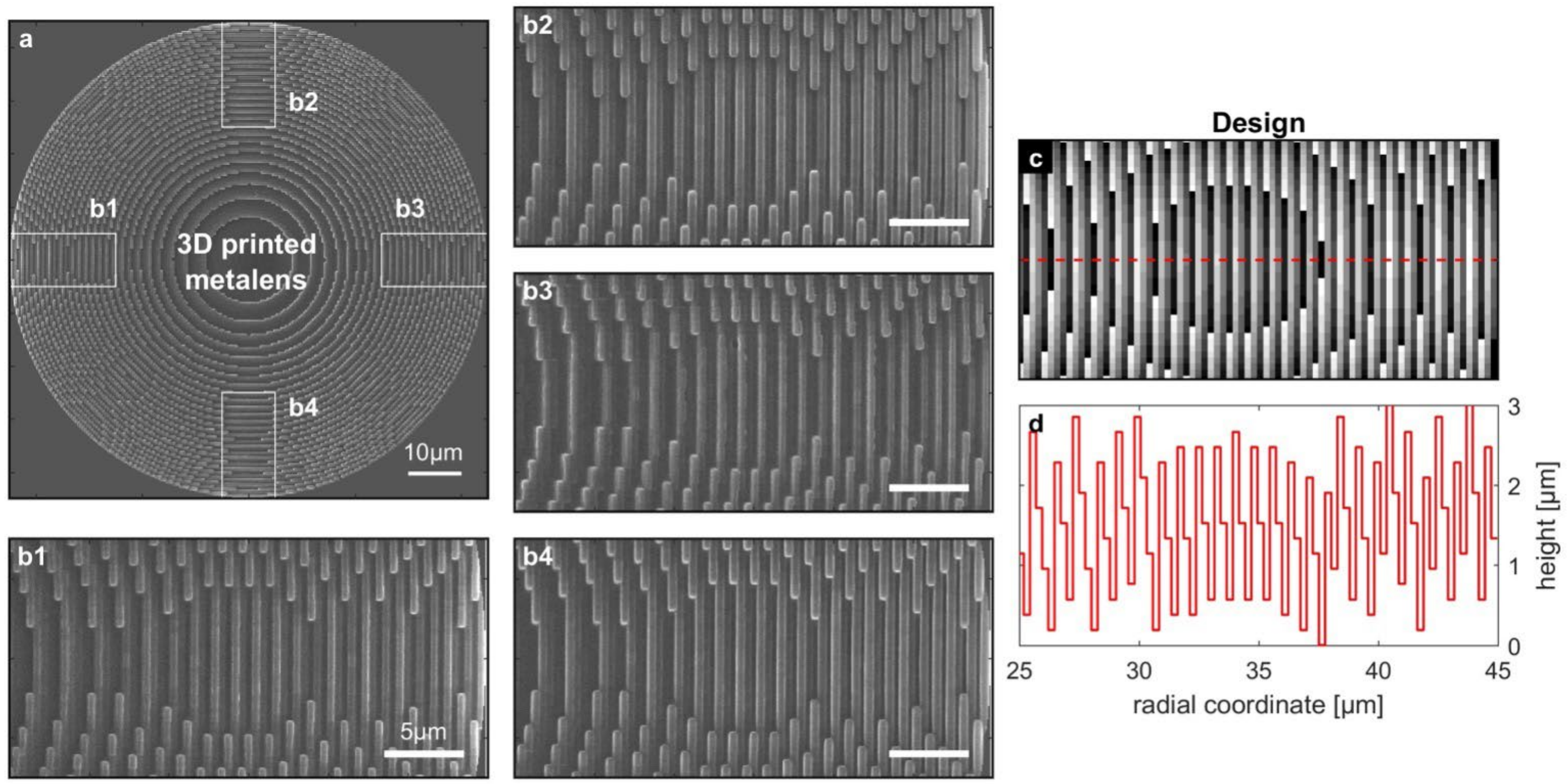

excellent agreement with design, NA ≈ 0.9

constant pitch, varying height < 3 µm, write time 1h, transmission > 50%

Full 3D optical trapping with a single device

Light: Science & Applications **10:57** (2021)

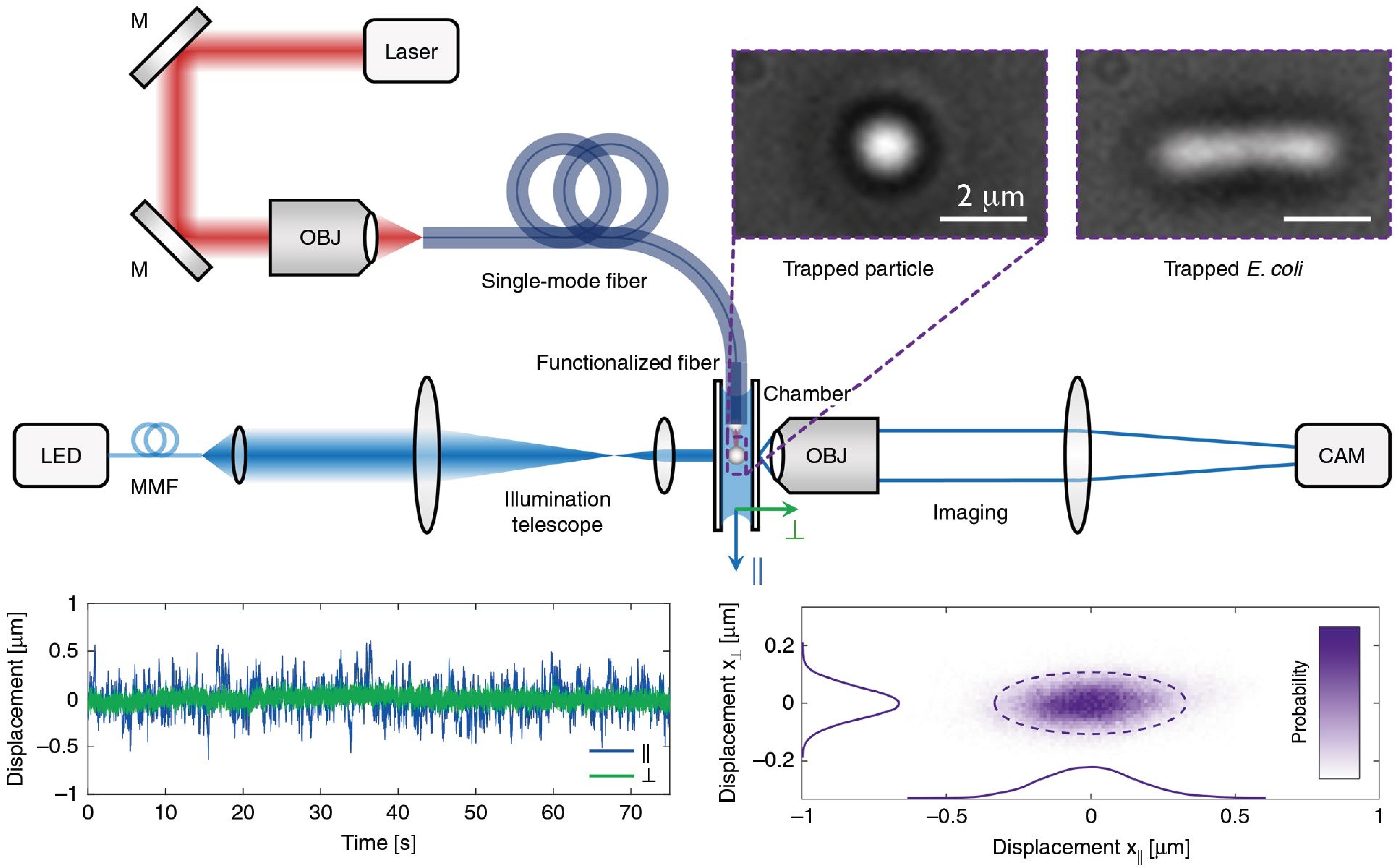

- trapping in water requires NA of at least 0.8
- laser diode operating at 660 nm with 37 mW
- motion of trapped objects recorded via Koehler illum imaging at 455 nm
- excellent trapping dynamics over timescales > 1 min
- displacement probability of silica sphere test object follows closely the focal spot intensity distribution

Determination of trap stiffness

Light: Science & Applications **10:57** (2021)

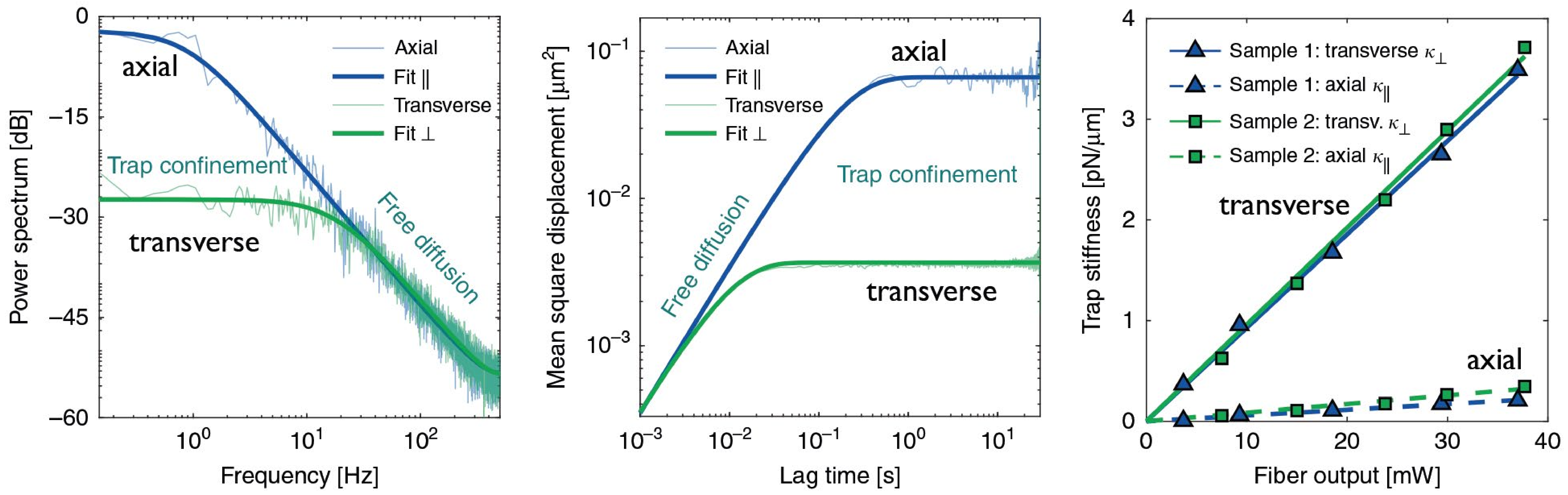

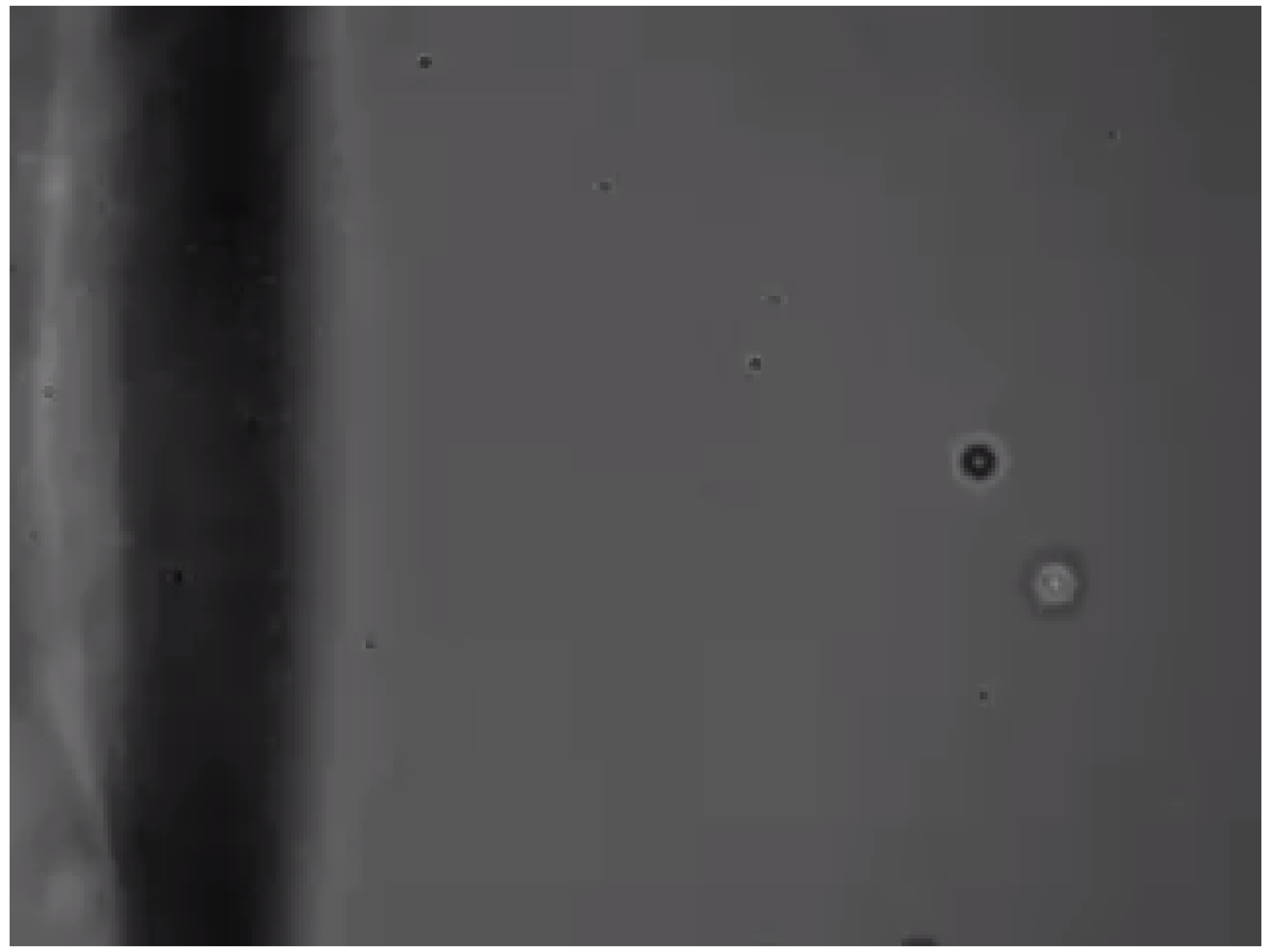

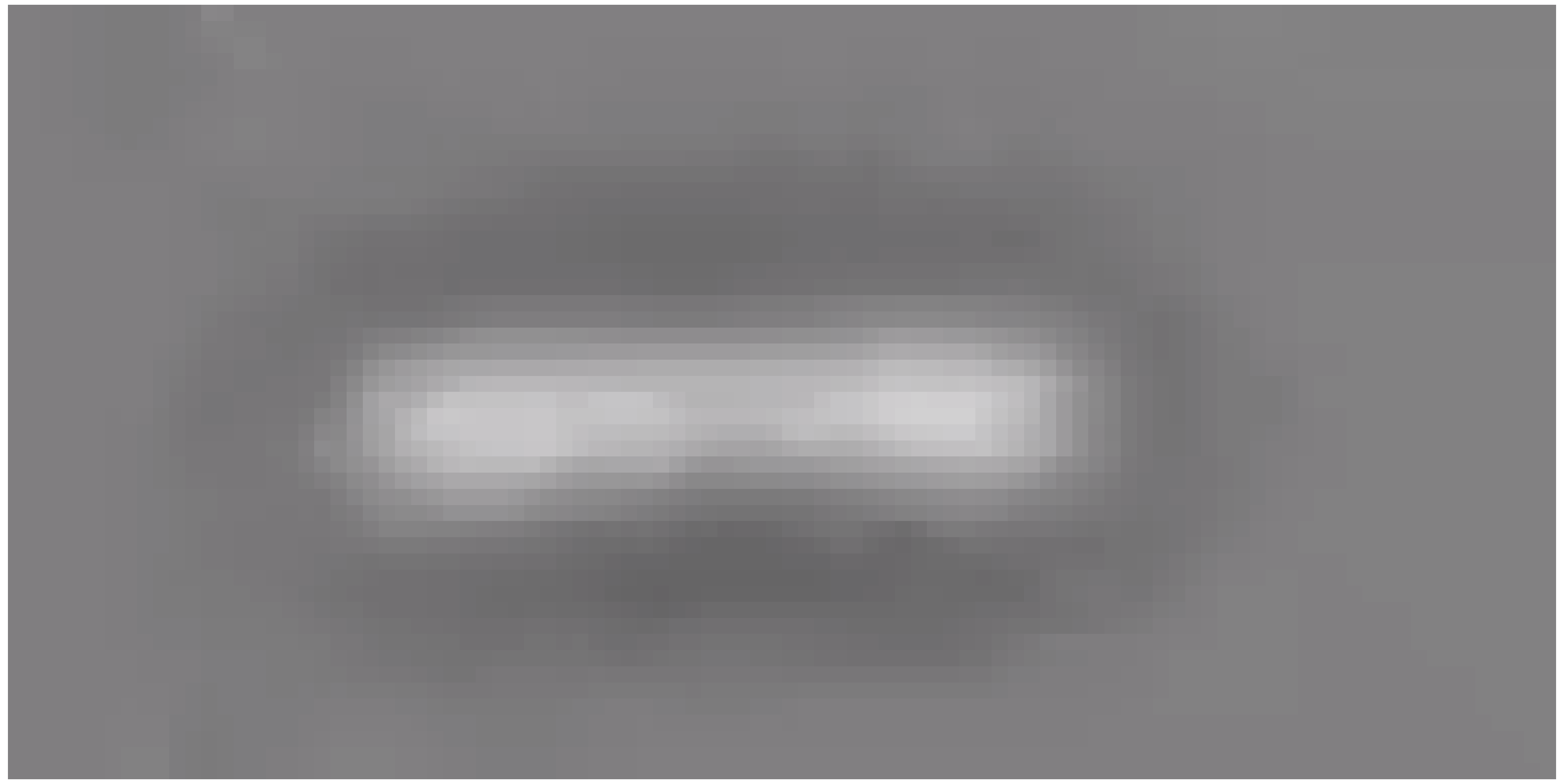

- power spectral density evaluation and mean-square-displacement analysis for determination of trap stiffness of representative displacement datasets
- ratio of transverse to axial trap stiffness as expected for elongated focus
- no particle drift on time scales > 1 min visible

Closing credits

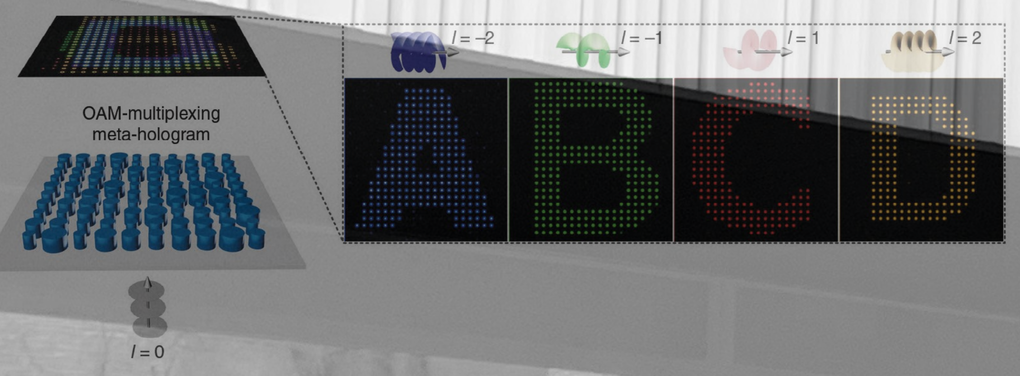

Haoran Ren
Patrice Genevet
Junsuk Rho

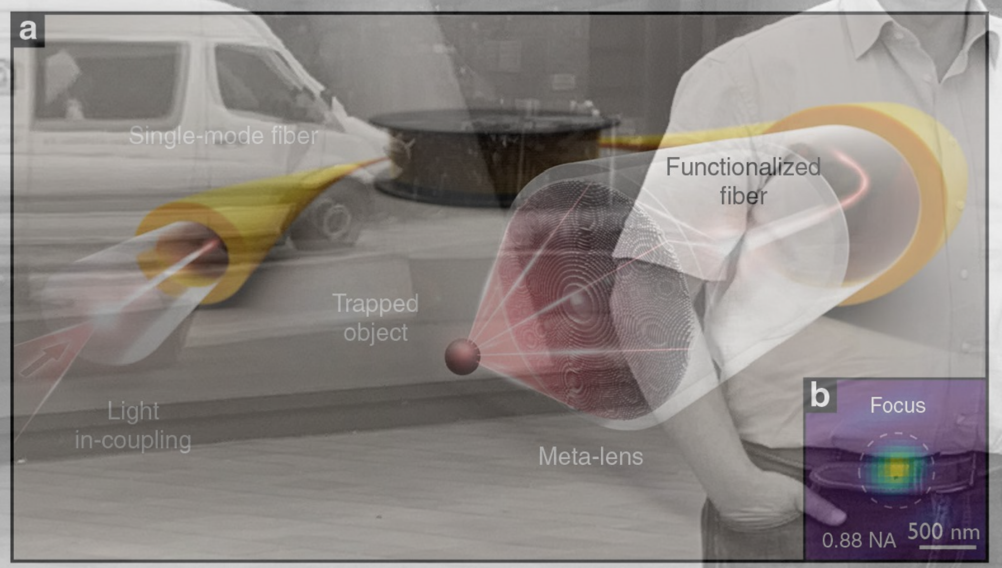

Markus Schmidt
Haoran Ren

Thank you for your attention

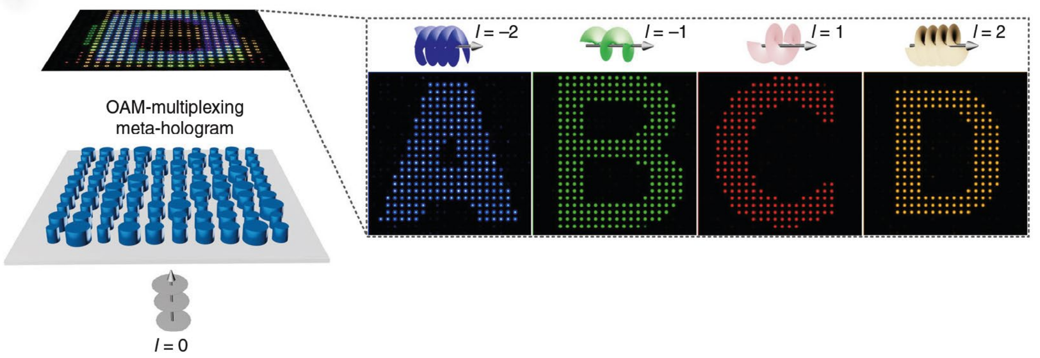

Metasurface holography

Nature Nanotechnology **15,** 948 (2020)
Nature Communications **10,** 2986 (2019)

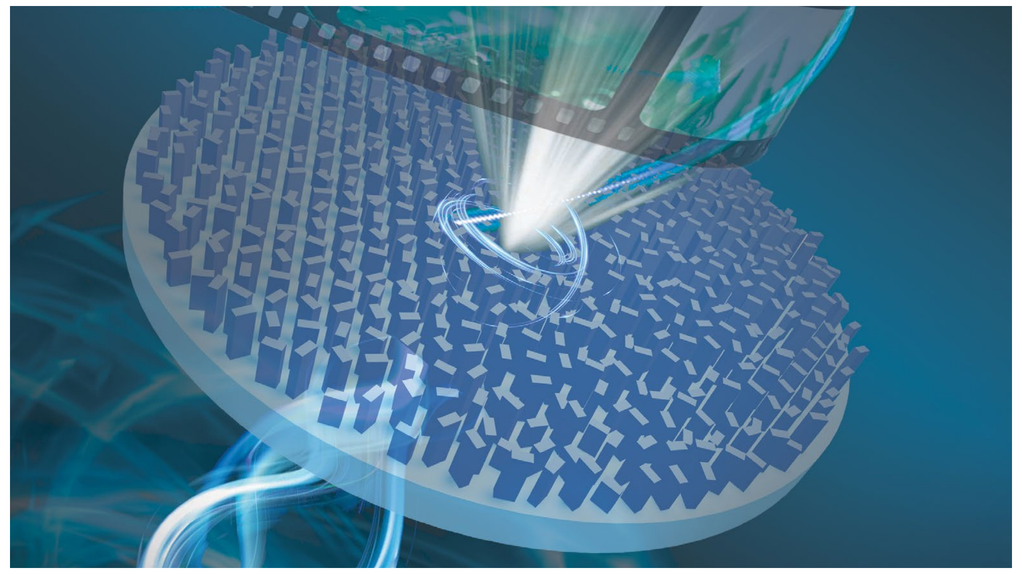

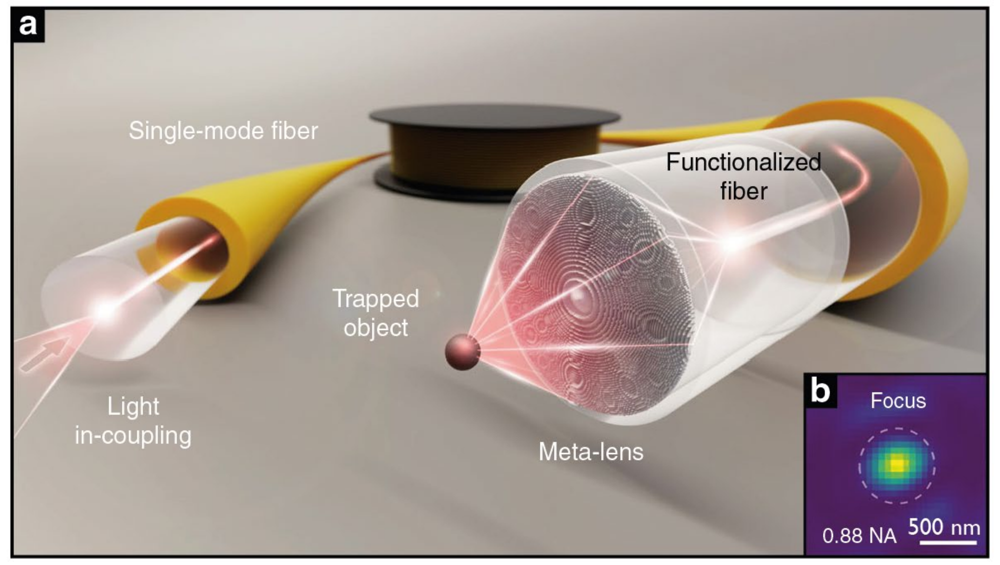

Meta-optics for optical fibre applications

*arxiv.org/abs/***2201.07158**
Light: Science & Applications **10:57** (2021)